RESERVOIR CHARACTERIZATION OF THE LOWER CRETACEOUS CEDAR MOUNTAIN AND DAKOTA FORMATIONS, NORTHERN UINTA BASIN, UTAH

by Brian S. Currie, Mary L. McPherson, William Hokanson, Justin S. Pierson, Mindy B. Homan, Thomas Pyden, William Schellenbach, Ryan Purcell, and David Nicklaus

OPEN-FILE REPORT 597
UTAH GEOLOGICAL SURVEY
a division of
UTAH DEPARTMENT OF NATURAL RESOURCES
2012

RESERVOIR CHARACTERIZATION OF THE LOWER CRETACEOUS CEDAR MOUNTAIN AND DAKOTA FORMATIONS, NORTHERN UINTA BASIN, UTAH

by Brian S. Currie[1], Mary L. McPherson[2], William Hokanson[1], Justin S. Pierson[1], Mindy B. Homan[1], Thomas Pyden[1], William Schellenbach[1], Ryan Purcell[1], and David Nicklaus[1]

[1]Department of Geology, 114 Shideler Hall, Miami University, Oxford, OH 45056
[2]McPherson Geologic Consulting, 3920 Fox, Casper, WY 82604

Cover photo: *Yellow and red mottled pebbly mudstone of the J-K paleosol complex near the Split Mountain 1 measured section.*

OPEN-FILE REPORT 597
UTAH GEOLOGICAL SURVEY
a division of
UTAH DEPARTMENT OF NATURAL RESOURCES
2012

STATE OF UTAH
Gary R. Herbert, Governor

DEPARTMENT OF NATURAL RESOURCES
Michael Styler, Executive Director

UTAH GEOLOGICAL SURVEY
Richard G. Allis, Director

PUBLICATIONS
contact
Natural Resources Map & Bookstore
1594 W. North Temple
Salt Lake City, UT 84114
telephone: 801-537-3320
toll-free: 1-888-UTAH MAP
website: mapstore.utah.gov
email: geostore@utah.gov

UTAH GEOLOGICAL SURVEY
contact
1594 W. North Temple, Suite 3110
Salt Lake City, UT 84114
telephone: 801-537-3300
website: geology.utah.gov

CONTENTS

FIGURES

TABLE

PLATES

RESERVOIR CHARACTERIZATION OF THE LOWER CRETACEOUS CEDAR MOUNTAIN AND DAKOTA FORMATIONS, NORTHERN UINTA BASIN, UTAH

by Brian S. Currie, Mary L. McPherson, William Hokanson, Justin S. Pierson, Mindy B. Homan, Thomas Pyden, William Schellenbach, Ryan Purcell, and David Nicklaus

INTRODUCTION

In the northern Uinta Basin of eastern Utah, sandstones in the Lower Cretaceous Cedar Mountain and Dakota Formations (CMD) are natural gas reservoirs. In recent years, the drilling of deep wells (>13,000 ft) in the northern part of the basin has demonstrated the potential of the CMD interval as a significant gas producer. Previous work on the controls of natural gas reservoirs in the CMD interval in eastern Utah include the stratigraphic/alluvial architecture of the CMD, paleoflow orientations of CMD fluvial systems, and petrophysical characteristics of the sandstone reservoirs (Currie et al., 2008a, 2008b; Dark et al., 2008). The CMD stratigraphic interval in eastern Utah contains at least four unconformity-bounded depositional sequences (Figure 1) (Young, 1960; Currie, 1997, 1998, 2002; McPherson et al., 2006; Currie et al., 2008b; Pierson, 2009). At each unconformity, fluvial systems were incised to varying degrees into older fluvial/alluvial strata. Subsequent valley filling and channel/flood-plain aggradation produced vertical and lateral juxtaposition of potential fluvial sandstone reservoirs of differing thickness, width, and connectivity. In addition, sandstone composition and diagenesis can vary between individual depositional sequences, significantly affecting reservoir porosities and permeabilities. The above effects result in highly complex hydrocarbon reservoirs that are difficult to characterize. The great depth of the CMD interval in the northern Uinta Basin adds additional uncertainty to play exploration and risk evaluation.

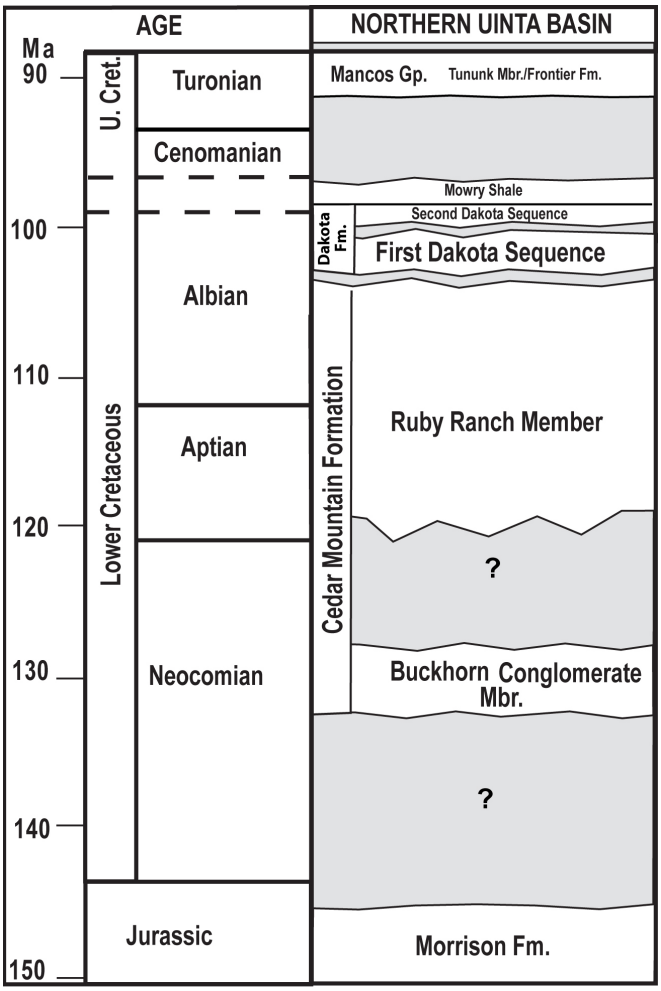

Figure 1. *Time-stratigraphic diagram of the Cedar Mountain and Dakota Formations in eastern Utah. Ages are based on CMD palynomorphs, marine fossils in the overlying Mancos Group, and regional stratigraphic relationships. Compiled from Stokes (1952), Molenaar and Cobban (1991), Kirkland and Madsen (2007), Scott et al. (2009); Pierson (2009), Sprinkel et al. (2012), and this report.*

In order to determine the primary controls on the distribution of economically viable CMD gas reservoirs, we have conducted an evaluation of well and outcrop data derived from the northern Uinta Basin. Our subsurface work has focused on an ~1000 mi^2 area in Uintah County, Utah, and SW Moffat County, Colorado (Figure 2). Additionally, CMD outcrops situated immediately north of the subsurface study area were used as surface control (Figure 2). Well completion reports and borehole logs from study area wells that penetrated the CMD were compared to determine the stratigraphic position of producing intervals. Outcrop gamma ray logs were acquired across the CMD interval to assist in developing a subsurface correlation model. Well logs from across the northern Uinta Basin were correlated within the context of CMD lithologic and palynology data derived from a core and outcrops in the study area. Isopach maps and structure contour maps of CMD stratigraphic units and intervals were constructed. Detailed reservoir architecture descriptions of the CMD were

generated at several outcrops. Porosity and permeability data from a CMD core were included in the study. Collectively, the components of the study were evaluated to determine the controlling factors on the occurrence of economic gas resources within the CMD in the northern Uinta Basin.

The results of each of the project components, as well as our conclusions as to the controls on economic gas production from the CMD interval, are described in greater detail below.

STRATIGRAPHY AND SEDIMENTOLOGY

In the study area, the CMD interval is Early Cretaceous age. The Upper Jurassic Morrison Formation lies below the CMD and the Lower-Upper Cretaceous Mowry Shale lies above. Figure 1 shows a time-stratigraphic diagram for the area. The CMD interval crops out in many places around the Uinta Basin and has been studied by many geologists. Significant contributors to the understanding of the CMD interval are Stokes (1952), Quigley (1959), Young (1960), Vaughn and Picard

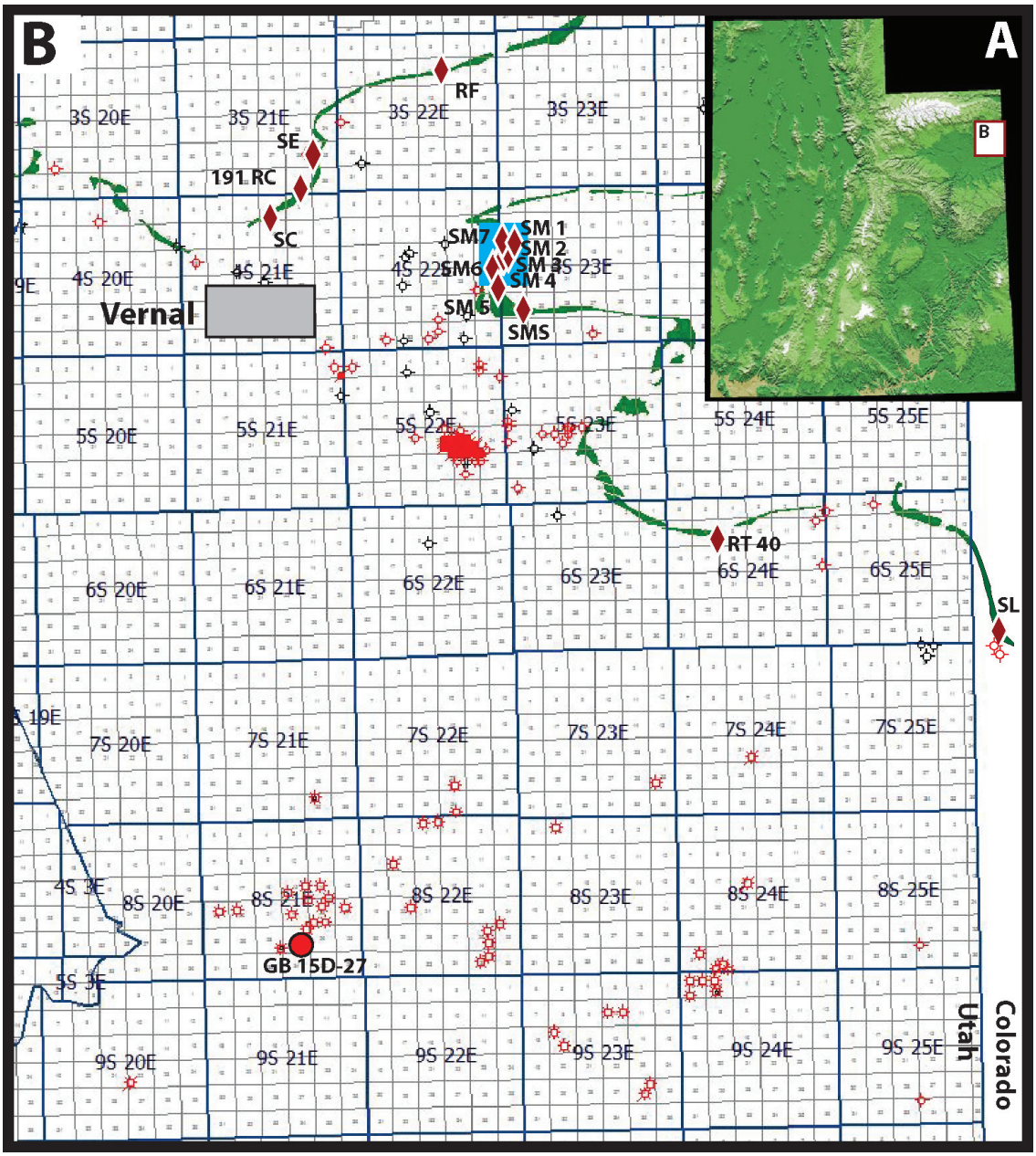

Figure 2. *Study area location maps. A) White rectangle shows study area location in eastern Utah (Inset B). B) Northern Uinta Basin study area. Green shading shows location of CMD outcrops. Red diamonds mark location of study outcrop measured sections referred to in text and figures. Measured section abbreviations are as follows 191 RC: 191 Road Cut; RF Red Fleet: RT 40: Route 40; SC: Steinaker Canal; SE: Steinaker Entrance; SL: State Line; SM 1-7: Split Mountain Sections 1 through 7; SMS: Split Mountain South. Blue rectangle shows approximate location of Split Mountain Anticline map area of Plate 2. Red well symbols mark location of wells used in the subsurface component of the study. Red circle shows location of Glen Bench 15D-27 well core.*

(1976), Ryer et al. (1987), Molenaar and Cobban (1991), Currie (1997; 1998; 2002), Kirkland and Madsen (2007), Currie et al. (2008a), Pierson (2009), and Sprinkel et al. (2012). The general lithologic characteristics and stratigraphic relationships of the Dakota Formation and Mowry Shale in the northern Uinta Basin, as well as bounding stratigraphic units, are discussed in more detail below. The following descriptions and interpretations represent a compilation of the above authors' observations, as well as our own. Measured sections of the CMD interval are shown in Plate 1.

Upper Jurassic Morrison Formation

The CMD stratigraphic interval is underlain by the Oxfordian-Tithonian (~154–147 Ma) Morrison Formation throughout the northern Uinta Basin. The upper part of the Morrison Formation is composed of the Brushy Basin Member. The Brushy Basin Member in the study area consists of ~230–330 ft of smectitic, alluvial/paludal mudstone, and chert-rich fluvial channel sandstone and conglomerate (Currie, 1998). The contact between the Brushy Basin Member and the overlying Cedar Mountain Formation represents the Jurassic-Cretaceous (J-K) unconformity in the region. In the eastern part of the study area, this contact is represented by an erosional contact at the base of the Buckhorn Conglomerate Member of the Cedar Mountain Formation. In the western part of the study area, the J-K unconformity is marked by a well-developed composite-paleosol complex formed beneath the Cedar Mountain Formation (Figure 3).

The J-K unconformity paleosol complex is preserved to differing degrees of completeness due to erosional truncation beneath fluvial/alluvial deposits of the overlying Ruby Ranch Member of the Cedar Mountain Formation. In most locations where it has been observed, only the lower levels of the pedogenic profile (i.e., B horizons) are preserved (Demko et al., 2004). In the study area, the paleosol is 5–30 ft thick, and consists of single to multiple, non-calcareous horizons of gray, red, and green mudstone. These mudstones are often sandy and contain floating granule-pebbles of rounded chert and quartzite. There is an up-section increase in degree of overall alteration of the original alluvial parent material as indicated by the abundance of observed pedogenic structures.

Individual paleosol horizons contain both angular-blocky and wedge-shaped peds that can exhibit clay films or slickensides. Horizons may also display abundant, irregularly shaped red-, gray-, yellow-, olive-, brown-, and green-colored mottles (Figure 3). Mottles range from <1 in to > 1 ft in diameter, and in some cases exhibit irregular cylindrical geometries that are oriented vertically to sub-horizontally. In some cases they display downward branching indicative of rooting. Most mottling is a result of oxidized or reduced iron within a relatively uniform, sandy-mudstone matrix. Some mottling is caused by the presence of irregular horizons or patches of iron and clay depletion/enrichment (Demko et al., 2004). Enriched zones can display broadly disseminated patches or small nodules (>3 inches diameter) of goethite and limonite, as well as concentrated patches of illite and smectite (K. Nicole, personal communication, 2009). Depleted zones are characterized by higher concentrations of silt and sand-sized particles, and appear bleached due to low abundances of reduced/oxidized iron. Depleted zones tend to be concentrated in the upper parts of the paleosol where they are least truncated, whereas enriched zones tend to be concentrated at lower levels (Demko et al., 2004).

Lower Cretaceous Cedar Mountain Formation

In the study area, the Neocomian-Albian Cedar Mountain Formation consists of the Buckhorn Conglomerate and Ruby Ranch Members (Currie, 1997;1998; Sprinkel et al., 2012). The Cedar Mountain Formation contains fluvial channel conglomerates and sandstones, and associated overbank lithologies. Detailed descriptions of each unit are listed below.

Buckhorn Conglomerate Member

The Buckhorn Conglomerate is only present in the eastern part of the study area. Surface exposures of the Buckhorn Conglomerate in the northern Uinta basin extend along a 20-

Figure 3. *Yellow and red mottled pebbly mudstone of the J-K paleosol complex near the Split Mountain 1 measured section (see Figure 2 for location).*

mile wide outcrop belt centered near Dinosaur, Colorado. The unit overlies bentonitic mudstones of the Brushy Basin Member, and is capped by the Ruby Ranch Member. The Buckhorn Conglomerate Member thins symmetrically from a maximum thickness of ~100 ft just east of the Utah-Colorado state line. Pinch-outs near Cliff Creek in Utah and Massadona, Colorado, define the western and eastern extent of exposed Buckhorn lithologies, respectively (Currie, 1998).

Where exposed, the Buckhorn Conglomerate Member consists primarily of upward-fining beds of conglomerate and sandstone (Figure 4). The unit also contains rare beds of intercalated mudstone. Conglomerates are clast-supported and dominated by pebble-sized clasts of gray, black, and white chert, with lesser amounts of sandstone, quartzite, quartz, and rare silicified wood and bone fragments. Conglomerate and sandstone beds in the Buckhorn Conglomerate Member are arranged in laterally and vertically amalgamated channel-form lenses that give the unit an overall sheet-like geometry. Individual Buckhorn channel complexes observed in outcrop have width to thickness ratios that range from 1000 to 3000 (Currie, 1998; Roca and Nadon, 2007).

Buckhorn Conglomerate Member sandstones consist of approximately equal proportions of chert and quartz grains, with less than 6% feldspar grains (Currie, 1998; Roca and Nadon, 2007). Sandstones and conglomerates are cemented primarily by calcite, although silica cement is also common. Fine-grained lithologies in the member consist of 3–16 ft thick beds of gray, green, and red bentonitic mudstone. Buckhorn mudstones contain common root and burrow traces and pedogenic/groundwater carbonate horizons. Mudstone in the unit is interpreted as overbank or abandoned-channel deposits preserved between individual channel complexes.

The Buckhorn Conglomerate Member is interpreted as being deposited by a northeast-flowing gravelly-sandy braided-fluvial system that was incised into the underlying Morrison Formation (Currie, 1997; 1998). Buckhorn fluvial deposits are oriented southwest-northeast in the northern part of the Uinta Basin (Currie, 1997; 1998). Lateral to this incised drainage, the J-K unconformity paleosol marks the contact between Morrison and Cedar Mountain Formations.

Although the Buckhorn Conglomerate contains no age-diagnostic fossils or volcanic ash horizons, it has historically been placed at the base of the Lower Cretaceous stratigraphic interval in eastern Utah (Stokes, 1952). Some workers have interpreted the Buckhorn Conglomerate as the uppermost member of the Upper Jurassic Morrison Formation (Aubrey, 1998; Roca and Nadon, 2007). Near the northwest edge of the Buckhorn paleo-drainage on the northern part of the San Rafael Swell, the paleosol interpreted as forming at the J-K unconformity is erosionally truncated by the Buckhorn Conglomerate (Demko et al., 2004). This superposition of the Buckhorn Conglomerate above the Jurassic-Cretaceous unconformity suggests an Early Cretaceous age of deposition of the unit. In addition, a possible Early Cretaceous ankylosaur has been identified from the Buckhorn Conglomerate near its type section on the San Rafael Swell (Kirkland, 2005), supporting the original Lower Cretaceous stratigraphic interpretation of Stokes (1952).

Ruby Ranch Member

In the eastern part of the outcrop study area, the Ruby Ranch Member overlies the Buckhorn Conglomerate Member. Where Buckhorn Conglomerate is absent, the Ruby Ranch Member rests directly above the unconformity paleosol at the top of the Morrison Formation. The Ruby Ranch Member consists of 80–150 ft of green, red, and gray mudstone. Mudstones contain abundant calcic and vertic paleosols and associated pedogenic-carbonate nodules and groundwater-calcrete beds in all but the upper parts of the member (Figure 5). Near the top of the Ruby Ranch Member, mudstones become increasingly bentonitic. The Ruby Ranch Member also contains lenticular fluvial channel deposits up to 20 ft thick. Sedimentary structures in Ruby Ranch sandstones include trough and planar cross-stratification, horizontal stratification, and ripple cross-lamination. Current indicators indicate an overall east

Figure 4. *A) Outcrop exposure of the Buckhorn Conglomerate Member 3 miles east of the study area near Dinosaur National Monument Headquarters, Dinosaur, Colorado. The Buckhorn is ~100 ft thick at this location. B) Close up photograph of typical Buckhorn chert-pebble conglomerate at the same locality as 4A.*

direction of paleoflow. The mineralogical composition and cements of these sandstones are similar to those in the Buckhorn Conglomerate Member (Currie, 1998).

The Ruby Ranch Member is interpreted as overbank and channel deposits of low sinuosity fluvial systems (Currie, 2002). Dinosaur fossils and U-Pb ages from authigenic carbonates and detrital zircons indicate a late Aptian-Albian (119–104 Ma) age of deposition (Kirkland and Madsen, 2007; Ludvigson et al., 2010; Sprinkel et al., 2012).

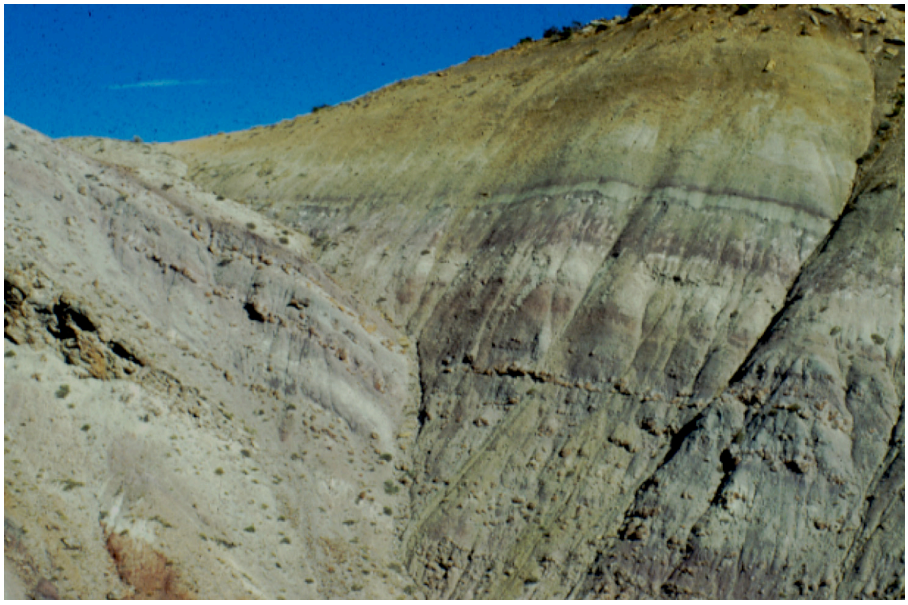

Figure 5. *Outcrop exposure of the Ruby Ranch Member of the Cedar Mountain Formation near the Split Mountain South measured section (see Figure 2 for location). Numerous calcareous paleosols and groundwater carbonate horizons crop out in the lower two-thirds of the photograph. Mudstone in the upper part of the outcrop is non-calcareous and increasingly smectitic towards the top of the unit. Stratigraphic thickness of the outcrop exposure is ~130 ft.*

Lower Cretaceous Dakota Formation

The Dakota Formation comprises fluvial channel, overbank, and marginal-marine deposits. In the northern Uinta Basin, outcrops of the Dakota Formation are 80–155 ft thick. Based on the architecture of fluvial sandstones, overbank mudstones, and associated marginal/shallow marine deposits, the Dakota Formation has been previously subdivided into two stratigraphic units (Vaughn and Picard, 1976; Currie, 2002; Currie et al., 2008b). Throughout the study area, the oldest Dakota sequence (Kd1) unconformably overlies overbank and fluvial channel deposits of the Albian-age Ruby Ranch Member of the Cedar Mountain Formation (Figure 2) (Vaughn and Picard, 1976, Currie, 2002; Kirkland and Madsen, 2007). The Second Dakota sequence (Kd2) unconformably overlies the lower Dakota sequence (Ryer et al., 1987; Currie, 2002; Currie et al., 2008a). In the northern Uinta Basin, the Kd2 is capped by the Mowry Shale (Molenaar and Cobban, 1991). Characteristics of both Dakota sequences are described below in more detail.

First Dakota Sequence

In the northern parts of the Uinta Basin, the First Dakota sequence (Kd1) is up to 130 ft thick and consists of channel-form sandstones and conglomerates, as well as fluvial overbank and marginal marine sandstones, siltstones, and mudstones. The Kd1 interval was deposited above a regional erosion surface incised as much as 60 ft into the underlying Cedar Mountain Formation (Plate 1, Figure 6).

The stratigraphically lowest parts of the Kd1, which occupy the area of deepest incision into the underlying Cedar Mountain Formation, consist of fluvial channel sandstones and conglomerates. Basal Kd1 channel deposits contain upward-fining beds of pebble-granule conglomerate and very coarse- to very fine-grained sandstone. Conglomerate clasts are made up of chert, sandstone, and quartzite (Figure 7), as well as rip-up clasts of underlying lithologies. Observed sedimentary structures include trough cross-stratification (Figure 8), horizontal bedding, and ripple cross-lamination.

Individual basal channel-form deposits are 10–50 ft thick with flow-perpendicular widths of <1000 ft. The lateral terminations of these channel bodies are commonly coincident with positive relief along the unconformity surface with the underlying Cedar Mountain Formation. Where these channel deposits pinch out laterally, poorly-sorted sandstone and carbonaceous mudstone of the Kd1 rests directly on gray smectitic mudstone of the Ruby Ranch Member (Figure 6).

The Kd1 above the basal channel deposits consists of up to 100 ft of mudstone, siltstone, and shale, with intercalated lenticular to tabular beds of sandstone and conglomerate, and rare bentonite beds. The lower 15–50 ft of this mud-dominated interval contains carbonaceous mudstone, siltstone, and shale containing abundant plant fragments. Tabular sandstone beds in the lower part of the sequence display both unidirectional and oscillatory ripples, and mud-draped ripple cross-lamination. Some sandstone and mudstone beds in this interval are extensively bioturbated and contain invertebrate trace fossils such as *Skolithos* and *Planolites* (Figure 9). A well core from the lower part of the Kd1 in the northern Uinta Basin (QEP Energy, Glen Bench 15D-27 in 27-8S-21E; API: 4304739662) contains a similar trace fossil assemblage, as well as abundant oyster fossils (see below). In addition, palynomorphs sampled from the lower part of the interval in outcrops and the QEP

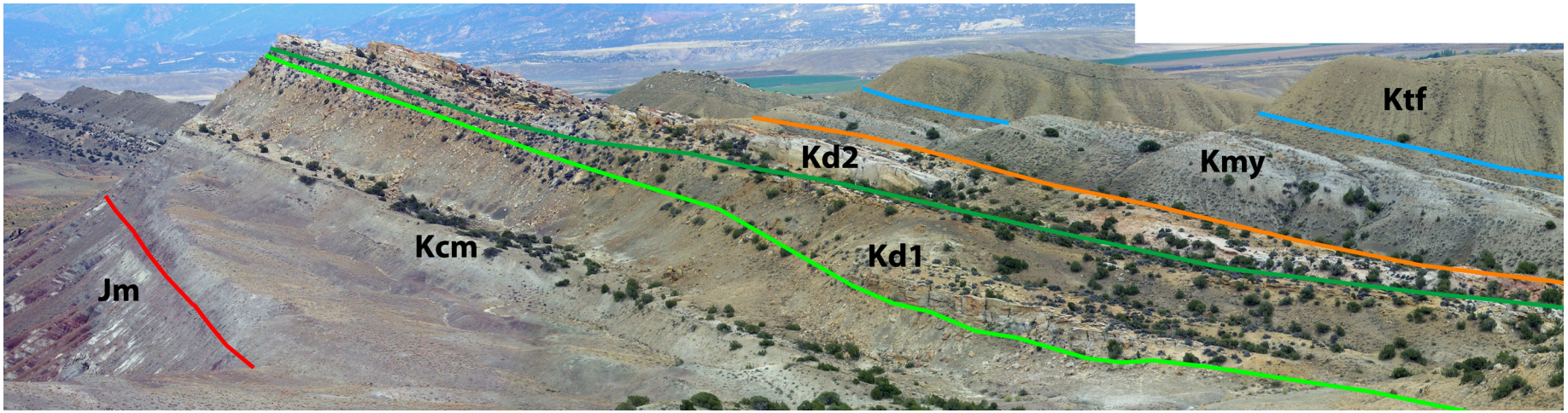

Figure 6. *Outcrop exposure of the CMD stratigraphic interval near the Split Mountain South measured section. Photo shows the lateral pinchout of First Dakota sequence (Kd1) fluvial channel deposits along the incised contact with the underlying Ruby Ranch member of the Cedar Mountain Formation (Kcm). Photo also shows incision of Second Dakota sequence (Kd2) fluvial deposits into estuarine/alluvial mudstones of the Kd1 sequence. CMD interval thickness at this location is ~ 260 ft. Jm= Jurassic Morrison Formation, Brushy Basin Member; Kmy= Cretaceous Mowry Shale; Ktf= Cretaceous Tununk Member, Frontier Formation. See Figure 2 for location.*

Figure 7. *Kd1 trough cross-stratified fluvial conglomerate and sandstone, 191 Road Cut section.*

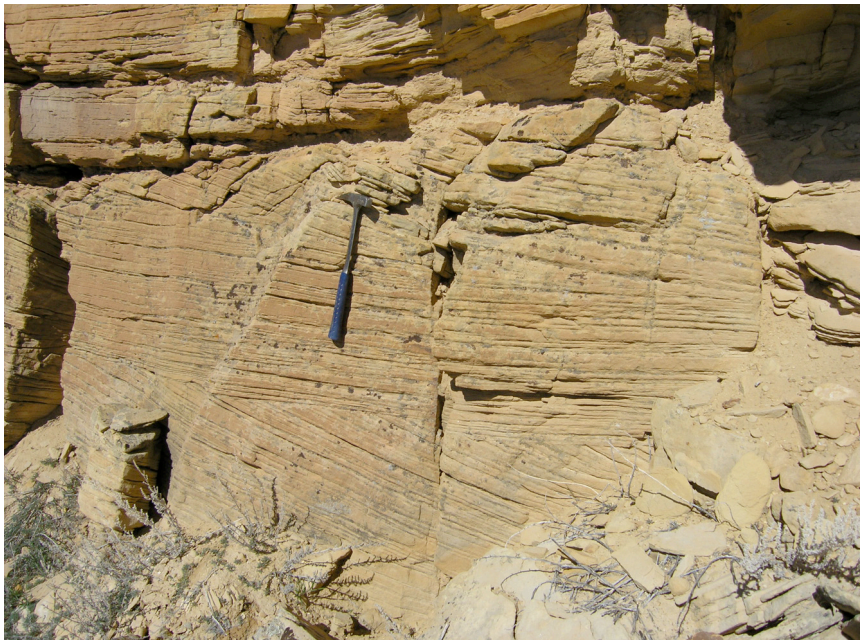

Figure 8. *Kd1 trough cross-stratified fluvial channel sandstone, SM 2 section.*

core contain both terrestrial and estuarine/marine palynomorphs (Sprinkel et al., 2012) (see below).

Channel-form sandstones and conglomerates up to 20 ft thick are also intercalated with the carbonaceous mudstones/shales and tabular sandstones of the lower Kd1. These channel bodies have lateral dimensions and internal lithofacies that are similar to the basal Kd1 channel deposits. An exception to these similarities are rare occurrences of herringbone cross-stratification (oppositely inclined-foreset orientations between adjacent trough cross-bed sets) observed in some Kd1 channel forms. Collectively, lithofacies and fossil data from the lower part of the Kd1 sequence indicate a marine influence on deposition (Sprinkel et al., 2012) The characteristics of this interval described above are consistent with deposition within the mid- to upper-reaches of a tidal estuary (see Dalrymple et al., 1992).

The upper parts of the Kd1 are dominated by fluvial channel and overbank deposits. Individual channel-form sandstones are between 10–50 ft thick and contain upward-fining beds of coarse- to very fine-grained sandstone. These channel forms are 250–1000 ft wide when measured perpendicular to paleoflow direction. In some cases, vertically amalgamated channel bodies form sandstone/conglomerate intervals that are up to 65 ft thick.

Overbank deposits in the upper parts of the Kd1 consist of beds of structureless to laminated, dark gray, smectitic, floodplain/paludal mudstone, and thin-bedded (<1.5 ft thick), horizontally-stratified/ripple cross-laminated crevasse splay sandstones and siltstones. In some instances, these Kd1 overbank deposits have been overprinted by pedogenic modification in the form of root traces, hydroximorphic mottling, and authigenic siderite/iron oxide accumulations.

In the study area, the Kd1 is middle to late Albian in age based on reported marine and terrestrial palynomorphs from the unit and a U-Pb radiometric age of 101.4 ± 0.4 Ma determined for zircon crystals sampled from a bentonite bed (Sprinkel et al., 2012).

Second Dakota Sequence

In the northern Uinta Basin, rocks of the Second Dakota sequence (Kd2) were deposited above a surface that is incised up to ~100 ft into underlying strata (Plate 1) (Currie, 2002). In rare instances, the entire Kd1 has been eroded and Kd2 rests directly on the Ruby Ranch Member (Plate 2 and Plate 3).

The Kd2 is 25–155 ft thick, and contains lithologies similar to the Kd1 (Plate 1). The lower part of the Kd2 is dominated by upward-fining fluvial channel sandstones and rare conglomerates. Sandstones range from coarse to very fine grained, but are dominantly medium grained. The lower parts of these beds contain boulder to granule sized rip-up clasts of underlying lithologies (Figure 10). Observed sedimentary structures in Kd2 channel sandstones include trough cross-stratification, horizontal bedding, and ripple cross-lamination (Figure 11). The upper parts of these fining upward intervals can contain thin interbeds of laminated carbonaceous mudstone and shale. These fine-grained caps likely reflect abandoned channel deposits.

Individual Kd2 channel-form sandstones are 16–50 ft thick and up to (~1650 ft) wide when measured perpendicular to paleoflow direction. In some localities, individual channel forms are laterally and vertically amalgamated into complexes that are up to 3300 ft wide and 100 ft thick. Paleocurrent orientations from trough cross-stratified Kd2 sandstones indicate primarily north-directed paleoflow (Vaughn and Picard, 1976; Currie, 2002; this study).

The top 1–50 ft of the Kd2 commonly displays evidence for a marine influence on deposition. In many localities, fluvial channel sandstones of the lower part of the Kd2 are sharply overlain by tabular-bedded, pebbly, medium- to fine-grained sandstone that contains both unidirectional and oscillatory flow ripples (Figure 12). Tabular beds also contain abundant

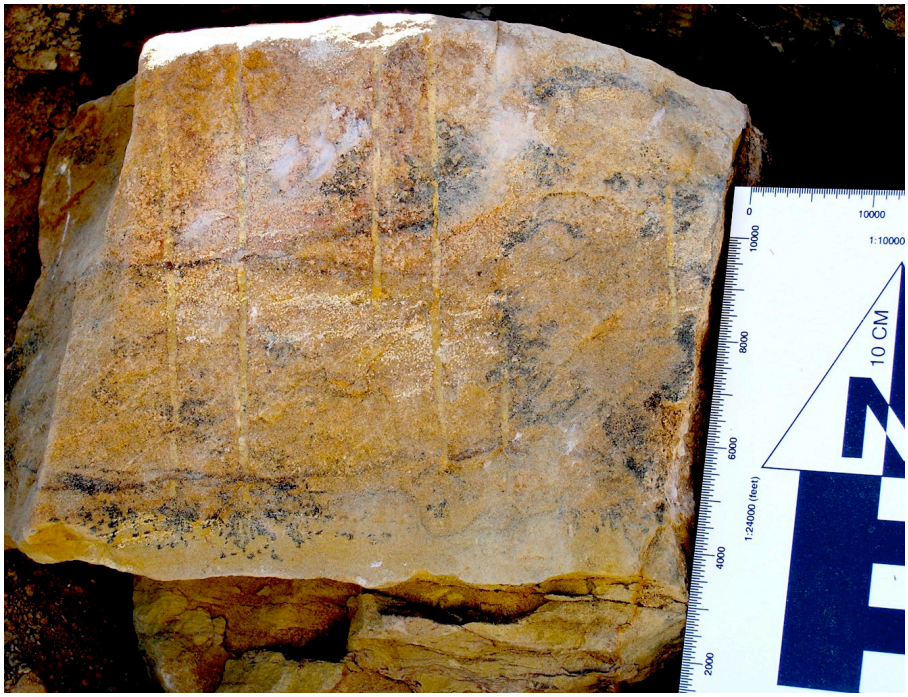

Figure 9. *Vertical* Skolithos *burrows in thin Kd1 tabular sandstone bed, SM 1 measured section.*

trough cross-stratification, and ripple cross-lamination. The upper parts of these beds are extensively bioturbated and contain invertebrate trace fossils including *Skolithos* and *Thalassinoides* (Figure 13). The upper part of the sequence is also associated with channel-form bodies that display well-developed herringbone cross-stratification (Figure 14). These tabular and channel-form beds likely reflect deposition in tidal sand flat and tidal channel depositional environments, respectively (see Boersma and Terwindt, 1981).

The upper part of the Kd2 also contains beds of black, brown, and gray carbonaceous mudstone and shale and rare yellow/white bentonite beds (Figure 15). Carbonaceous lithologies contain abundant plant fragments and leaf fossils, as well as abundant terrestrial palynomorphs (see below). These beds were likely deposited in a low energy marine embayment or the central basin of a tidal estuary (Dalrymple et al., 1992).

The Kd2 is capped in most localities by beds of conglomerate and pebbly, medium- to very fine-grained sandstone that are up to 10 ft thick. Conglomerates are horizontally to trough cross-stratified. In many localities, conglomerate beds display symmetrical ripples with wavelengths of up to 6 ft and amplitudes of up to 6 in (Figure 16). Sedimentary structures observed in the sequence-capping sandstone beds include trough cross-stratification, ripple cross-lamination, hummocky cross-stratification and symmetrical ripples. Sandstone beds also contain flaser-laminated and wavy-bedded intercalations of carbonaceous shale, as well as invertebrate trace fossils including *Skolithos*, *Planolites*, *Thalassinoides*, *Ophiomorpha*, and *Arenicolites*. Palynomorphs sampled from the interbedded shales contain abundant marine palynomorphs (see Palynology section below).

These uppermost conglomerates and sandstones in the sequence were likely deposited by large storm and/or tidal currents in a tidal/wave-dominated shelf system during the marine transgression that preceded deposition of the overlying Mowry Shale (Pierson, 2009). In the study area, the Kd2 is late Albian in age based on marine and terrestrial palynomorphs identified from the unit (see below).

Figure 10. *Boulder-size mudstone rip-up clast, recessed due to erosion, near the base of base Kd2, SM 2 measured section.*

Figure 11. *Trough cross-stratified Kd2 fluvial deposits, SM 2 measured section.*

Figure 12. *Sharp contact between Kd2 fluvial channel facies and overlying tabular-bedded upper Kd2 tidal sandstone near the SM 3 measured section. Tabular-bedded sandstone contains both unidirectional and oscillatory ripples.*

Figure 13. Thalassinoides *burrows, upper Kd2 tidal sandstone, SM 3 measured section.*

Figure 14. *Herringbone cross-stratification, upper Kd2 tidal sandstone near the 191 Road Cut measured section.*

Mowry Shale

In the outcrops of the northern Uinta Basin, the Mowry Shale is 35–115 ft thick and is composed of black, gray, and silver marine shale, mudstone, and siltstone with multiple interbedded bentonite beds (Figure 17). The Mowry Shale is interpreted as being deposited in a marine shelf environment at or below storm wave base (Byers and Larson, 1979; Davis and Byers, 1989). The lower 30–50 ft of the Mowry Shale in the study area consist of black, fissile shale and siltstone with rare beds of medium- to very fine grained, hummocky cross-stratified sandstone. The upper parts of the unit consist of hard, silver-gray weathering, siliceous shale and siltstone (Sharp, 1963). Both the lower and upper parts of the Mowry Shale contain abundant disseminated plant material and fossil fish scales/bone fragments, and rare ammonite fossils (Sharp, 1963; Molenaar and Wilson, 1990). The fissile and siliceous shales in the outcrops of the Mowry Shale in the northern Uinta Basin correlate with upward-coarsening shoreface siltstones and sandstones in the subsurface portion of the study area (Pierson, 2009).

In the northern Uinta Basin, the top of the Mowry Shale is placed at the sharp contact between the dark gray-silver siliceous shale of the upper Mowry and black, fissile, marine shales of the Tununk Shale Member of the Frontier Formation (Figure 17) (Molenaar and Wilson, 1990).

Based on age-defining ammonites sampled from the Mowry Shale in the study area, the unit has been interpreted as being deposited at ~98 Ma during early Cenomanian time (Molenaar and Wilson, 1990; Pierson, 2009). Palynomorphs sampled from the Mowry Shale, however, indicate a late Albian age of deposition (see Palynology section). This discrepancy is due to ongoing debates over how the current age of the Albian-Cenomanian boundary (~99 ma; Gradstein et al., 2004) corresponds with global palynostratigraphic age determinations (Oboh-Ikuenobe et al., 2007; Scott et al., 2009).

PALYNOLOGY

As part of this study, 13 samples were processed and analyzed for fossil palynomorphs. Samples were collected from outcrop samples of carbonaceous mudstones and shale of the Dakota Formation and Mowry Shale. Outcrop samples were taken from 1–3 in thick beds of unweathered mudstone that were devoid of modern plant material. Approximately 100–200 grams of mudstone were collected at each outcrop sample horizon, but only 3–5 grams were processed for palynomorphs. Additionally, the palynology results from an analysis of the four mudstone samples from the Glen Bench 15D-27 well (API: 43047396620000) in 27-8S-21E were obtained from QEP Resources. Sample locations are shown in Figure 2.

Of the seventeen samples analyzed, fifteen yielded identifiable fossil pollen, spores, or dinoflagellate cysts. Nine were age-diagnostic. All analyses, including the core samples, were

Figure 15. *Yellow bentonite bed and interbedded carbonaceous shale in the upper Kd2 estuary deposits, Red Fleet measured section. Bentonite bed is ~1.5 ft thick.*

Figure 16. *Wave-rippled gravel at base of the upper Kd2 sequence marine sandstone, Steinaker Entrance measured section. Photo by Robert Ressetar, Utah Geological Survey.*

conducted by Gerald Waanders, consulting palynologist. A summary of the analyzed samples is presented below. A full list of identified taxa, estimated visual Thermal Alteration Index (T.A.I.) values, kerogen content, interpreted stratigraphic age, and paleoenvironment interpretations for each sample can be found in Appendix A.

Figure 17. *Outcrop of the Mowry Shale and overlying Tununk Shale/Frontier Formation, Steinaker Entrance measured section. Photo by Robert Ressetar, Utah Geological Survey.*

Outcrop Data

Route 40 Section (Sec. 8, T. 6S, R. 24E)

A sample from the Kd1 (RT40 30) and a sample from the Kd2 (RT40 42) were taken from the Route 40 Section (Figure 2). Organic recoveries from the Kd1 sample were very good and consisted mostly of mixed woody and cuticular kerogens. Palynomorph recoveries were land-derived indicating a fluvial/deltaic paleoenvironment. Organic recoveries from the Kd2 sequence sample were good and consisted of mixed amorphous, woody, and cuticular kerogens. Palynomorph recoveries were land-derived indicating a swamp/deltaic environment. The visual T.A.I. values for both samples are 0.3–0.4% estimated vitrinite reflectance. No age-diagnostic palynomorphs were identified in either sample.

Split Mountain South Section (Sec. 30, T. 4S, R. 23E)

A sample from the Kd2 (SMS 90) and a sample from the base of the Mowry Shale (SMS 116) were taken from the Split Mountain South Section (Figure 2). Organic recoveries from the Kd2 sample were very good and consisted mostly of woody kerogens (70%). Palynomorph recoveries were land-derived and indicated a swamp/deltaic depositional paleoenvironment. A late Albian age of the sample is indicated by the presence of the trilete spores *Neoraistrickia robusta*, *Pilosisporites trichopapillosus*, *Trilobosporites crassus*, and *Trilobosporites marylandensis* (G. Waanders, personal communication, 2010).

The Mowry Shale sample was taken from the very base of the unit in the Split Mountain South Section and contained both marine microplankton and land-derived spores and pollen. Organic recoveries from the sample were good and consisted of primarily woody kerogens (70%), with subequal proportions of amorphous and cuticular kerogens. Age-diagnostic palynomorphs in the sample consist of *Appendicisporites jansonii* and *Neoraistrickia robusta* and the dinoflagellate cysts *Aptea polymorpha*, *Chichaouadinium vestitum*, *Ovoidinium scabrosum* and *Ovoidinium verrucosum*. This assemblage indicates a late Albian age of deposition. The diverse marine microplankton assemblage in the sample indicates a nearshore marine depositional environment.

Split Mountain 4 Section (Sec. 18, T. 4S, R. 23E)

One sample from the Kd1 (SMA4 19) and two samples from the Kd2 (SMA4 41, SAM4 52) were taken from the Split Mountain 4 Section (Figure 2). Organic recoveries from all samples were good to very good and consisted mostly of woody kerogens in the lower two samples, and mixed woody, amorphous, and cuticular kerogens in the uppermost sample (SAM4 52). Palynomorph recoveries were land-derived indicating a fluvial/deltaic/swamp paleoenvironment. The visual T.A.I. values for all samples are 0.3–0.4% estimated vitrinite reflectance. No age-diagnostic palynomorphs were identified.

Red Fleet Section (Sec. 10, T. 3S, R. 22E)

A sample from the Kd1 (RF 92), Kd2 (RF 107), and Mowry Shale (RF 108.5) were taken from the Red Fleet Section (Figure 2 Plate 1). Organic recoveries from the lower Dakota sequence sample were very good and consisted mostly of woody kerogens. Palynomorph recoveries were land-derived indicating a fluvial/deltaic paleoenvironment. A late Albian age of the sample is indicated by the presence of the trilete spores *Neoraistrickia robusta*, *Pilosisporites trichopapillosus*, and *Pilosisporites verus* (G. Waanders, personal communication, 2010).

Organic recoveries from the Kd2 sample were good and consisted of mixed amorphous (40%), cuticular (30%), and woody (30%) kerogens. Palynomorph recoveries were all nonmarine. Identified taxa indicate an undifferentiated late

Albian-early Cenomanian age of deposition. The presence of the green algae *Schizosporis reticulates* and Zygmataceae, as well as the relatively high amorphous kerogen in the sample, suggests deposition within a swamp/shallow lacustrine paleoenvironment.

The Mowry Shale sample was taken from the very base of the unit in the Red Fleet Section (Plate 1) and contained both marine microplankton and land-derived spores and pollen. Organic recoveries from the sample were good and consisted of mixed amorphous, cuticular, and woody kerogens. Age-diagnostic palynomorphs in the sample consist of the trilete spore *Neoraistrickia robusta* and the dinoflagellate cysts *Luxadinium propatulum* and *Subtilisphaera perlucida*, indicating a late Albian age of deposition. The diverse marine microplankton assemblage in the sample indicates a nearshore marine depositional environment.

Steinaker Entrance Section (Sec. 26, T. 3S, R. 21E)

A sample collected from directly above a wave-rippled gravel bed in the upper part of the Kd2 at the Steinaker Entrance Section (Figure 2) contained both marine microplankton and land-derived spores and pollen. Total organic recovery in the sample was very good and consisted of mostly woody kerogens (70%). The visual T.A.I. values for all samples are 0.3–0.4% estimated vitrinite reflectance. Age-diagnostic palynomorphs in the sample consisted of the dinoflagellate cysts *Chichaouadinium vestitum* and *Subtilisphaera perlucida* (Appendix A), indicating a late Albian age of deposition. The marine microplankton assemblage in the sample indicates a likely estuarine depositional environment.

Core Data

Glen Bench 15D-27 (API:4304739662), Sec. 27, T. 8 S, R. 21E

Four core samples from the Glen Bench (GB) 15D-27 well in central Uintah County yielded identifiable palynomorphs (Appendix A). The samples were derived from the lower part of the Kd1. All samples yielded good to very good organic recoveries and were dominated by woody kerogens. The presence of the dinoflagellate cyst *Microdinium ornatum* in sample 16177.1 indicates a marine influence on deposition.

The upper three samples (16170.7, 16177.1, and 16178.8) yielded a palynomorph assemblage indicative of a late Albian age of deposition based on the occurrences of *Peromonolites allensis*, *Neoraistrickia robusta*, and *Peromonolites allensis*. There were no age-diagnostic palynomorphs in the stratigraphically lowest sample (16188.2). Visual T.A.I. values for all samples were 0.6–0.7% estimated vitrinite reflectance.

Stratigraphic Implications

The palynology data presented above help refine previous interpretations of the regional stratigraphy of the CMD interval. Based on age-diagnostic palynomorphs present in sampled intervals, both the Kd1 and Kd2 as well as the overlying Mowry Shale are late Albian in age. The late Albian age of the Mowry Shale reported here, however, is older than the early Cenomanian age of the unit interpreted from ammonite fossils identified in the Uinta Mountains region (*Neogastroplites cornutus* and *Neogastroplites americanus*), and radiometric dates that bracket the age of the Mowry Shale in the Western Interior (97.2–98.5 Ma) (Molenaar and Wilson, 1990; Obradovich, 1993).

The late Albian palynomorph taxa identified as part of the current study, however, have been identified in the Mowry Shale in Wyoming and Montana where they are intercalated with the same ammonites and bracketed by the same radiometric dates used to interpret an early Cenomanian age for the Mowry Shale (Oboh-Ikuenobe et al., 2007). The discrepancy in interpreted age reflects the ongoing debate over how the age of the Western Interior *Neogastroplites* fauna and the currently interpreted age of the Albian-Cenomanian boundary (~99 Ma; Gradstein et al., 2004) correspond with global palynostratigraphic age determinations (Oboh-Ikuenobe et al., 2007, Scott et al., 2009). In that sense, the palynology-based age interpretations presented above are consistent with previous work on the biostratigraphy of the Mowry Shale, and indicate that the Mowry interval in the Uinta Mountain region was likely deposited ~98–97.5 Ma (Scott et al., 2009).

STRATIGRAPHIC ARCHITECTURE

Outcrop exposures of the CMD were examined along the western plunge of the Split Mountain anticline in the northern part of the study area (Figure 2) in order to define the internal structure and lithological variability of potential reservoir sandstones. As part of this study, the stratigraphic contacts of the Cedar Mountain Formation and the two Dakota sequences (Kd1 and Kd2) were mapped at the scale of 1:5000 (Plate 2). Where possible, the lateral dimensions of internal CMD facies assemblages and sandstone bodies were documented. In addition, a photomosaic of well exposed, near vertical outcrops of the CMD interval were constructed to delineate the geometry of bounding surfaces separating individual sandstone bodies and facies assemblages (Plate 3). Paleocurrent indicators were measured during both the outcrop and photomosaic mapping exercises to document CMD paleoflow orientations.

In the Split Mountain anticline map area, the Cedar Mountain Formation is ~150 ft thick and is made up entirely of the Ruby Ranch Member (Plate 1). The J-K unconformity paleosol separating the Cedar Mountain and Morrison formations is well-developed in this area (Figure 3). The Ruby

Ranch Member at Split Mountain consists primarily of gray, green, and red mudstones that contain abundant carbonate nodules in all but the upper ~10–20 ft of the member (Plate 1, Plate 3). Lenticular fluvial channel deposits up to 20 ft thick are also exposed along the outcrop (Plate 3). These channel bodies have flow-perpendicular widths of between 250 and 650 ft. Paleocurrent orientations indicate a N-NE direction of paleoflow (Average 25°, n=25).

The First Dakota Sequence (Kd1) in the map area is up to 90 ft thick. In most parts of the map area, Kd1 carbonaceous mudstones/shales and poorly sorted sandstones directly overlie the Cedar Mountain Formation. These carbonaceous beds were likely deposited in alluvial overbank and estuarine environments (see Sedimentology/Stratigraphy section above). Both nonmarine and marine palynomorphs have been reported from near the base of the Dakota Formation near the SM 6 measured section (Plate 1, Plate 2) (Sprinkel et al., 2012).

Although mudstone is commonly found at the base of the unit, channel-form sandstones and conglomerates dominate the lower part of the Kd1 interval in the area of the outcrop photomosaic (Plate 3). In some areas, these channel deposits cut down through the underlying carbonaceous deposits and rest directly on the Cedar Mountain Formation. Kd1 channel deposits in the outcrop exposure consist of an overall upward-fining sequence of coarse- to fine-grained sandstones. Although poorly exposed and erosionally truncated, individual basal channel-form deposits are between 10–20 ft thick with flow-perpendicular widths of <300 ft. Vertical and lateral amalgamation of these channel forms creates an overall sheet like geometry of the lower sandstone in the outcrop exposure. Sedimentary structures in the lower Dakota include trough- and planar-cross stratification, horizontal stratification and ripple-cross lamination. Paleocurrent orientations indicate a NNW direction of paleoflow (Average 342°, n=60).

The uppermost parts of the Kd1 interval in the map area and exposed in the outcrops of the photomosaic consist of carbonaceous estuarine and alluvial overbank deposits similar to those at the base of the interval. Tabular-sandstone beds in this interval display mud-draped ripple cross-lamination. Both sandstone and mudstone beds in the upper Kd1 are extensively bioturbated and contain invertebrate trace fossils such as *Skolithos* (Figure 9) and Planolites, as well as root traces.

In the central part of the Split Mountain anticline map area, the upper fine-grained parts of the Kd1 interval are erosionally truncated beneath the Second Dakota Sequence (Kd2). The progressive N-S erosional truncation of the Kd1 is discernable in Plate 3. In this area, Kd2 deposits symmetrically thicken from about 30 ft thick near both the SM 4 and SM 7 measured sections to ~155 ft near the SM 3 measured section (Plate 1). South of the SM 3 section, the entire Kd1 has been eroded and Kd2 deposits rest directly on the upper parts of the Ruby Ranch Member (Plate 2, Plate 3). The contact between the Kd2 and the underlying Kd1 deposits is sharp with no observed interbedding between the coarse- and fine-grained lithologies (Figure 18). The thin Kd2 to both the north and south consists of only the upper tabular-bedded tidal/estuarine sandstones and the overlying carbonaceous mudstones and shales.

In the thick, deeply incised area, Kd2 deposits are dominated by amalgamated, upward-fining, channel-form sandstones and conglomerates that are up to 30 ft thick and ~1500 ft wide perpendicular to paleoflow direction (Plate 3). The base of each channel body contains abundant chert/quartzite granules and pebbles, as well as granule- to boulder-sized mudstone and sandstone rip-up clasts. Internally, channel bodies fine upward from coarse/medium to fine-grained sand. In some instances, channels are capped by interbeds of laminated carbonaceous mudstone and shale, likely deposited following channel abandonment. Sedimentary structures observed in Kd2 channel sandstone include trough and planar cross-stratification, horizontal stratification and ripple cross-lamination. Kd2 Paleocurrent orientations taken from the incised area indicate a WNW direction of paleoflow (Average 298°, n=154) (Plate 2).

The area where the Kd2 symmetrically thickens is interpreted as a ~3300 ft wide paleovalley that was incised into underlying Kd1 deposits during the development of the unconformity separating the two sequences. The mapped margins of the paleovalley are parallel to Kd2 fluvial channel paleoflow indicators recorded in the amalgamated fluvial channel complex within the paleovalley margins (Plate 2). The Split Mountain outcrop exposure in the photomosaic contains the central and northern portion of the interpreted Kd2 paleovalley (Plate 2, Plate 3).

Tabular to broadly lenticular beds of tidal flat sandstone cap Kd2 fluvial paleovalley deposits in the studied outcrop exposure. These same sandstones directly overlie Kd1 deposits near the SM 5 and SM 6 measured sections in the southern part of the map area and the SM 7 measured section in the north part of the map area (Figure 18A, Plate 1, Plate 2). These sandstone beds are up to 10 ft thick, have erosional bases, and consist of pebbly, medium- to fine-grained sandstone that contains both unidirectional and oscillatory ripples, as well as abundant trough cross-stratification, and ripple cross-lamination. The upper parts of these beds are extensively bioturbated and contain invertebrate trace fossils (Figure 13). In the central part of the studied outcrop exposure, the lowermost tidal sandstones are truncated by a channel-form sandstone similar to those in the underlying fluvial-dominated interval. This suggests that the upper parts of the Kd2 paleovalley have been tidally influenced. Collectively, these tabular-lenticular sandstones produce a continuous sheet-like sand body that is up to 25 ft thick. The tabular sandstone interval is capped

by carbonaceous estuarine mudstone, shale, and bentonites (Plate 1, Plate 2, Plate 3).

The top of Kd2 interval in the Split Mountain anticline map area is marked by a ~3–10 ft thick interval of interbedded marine conglomerate, sandstone, and shale. Conglomerates in this interval consist of granule- to pebble-size clasts of chert and quartzite and are horizontally to trough cross-stratified. Interbedded sandstones are medium to fine grained and contain sedimentary structures including trough cross-stratification, ripple cross-lamination, hummocky cross-stratification and symmetrical ripples. These sandstone beds also contain flaser-laminated and wavy-bedded intercalations of carbonaceous shale, as well as invertebrate trace fossils including *Skolithos*, *Planolites*, *Thalassinoides*, and *Arenicolites*. This upper sandstone is laterally traceable across the entire outcrop exposure and throughout the surrounding map area at the contact with the overlying Mowry Shale (Plate 1 and Plate 2).

Paleocurrent Orientations

Over 1300 paleocurrent orientations were measured from outcrop exposures of the CMD fluvial and tidal channel sandstone and conglomerates throughout the study area (Figure 19). Orientations were measured from the dip direction of foresets in planar and trough cross-stratified sandstones, or from the orientation of trough axes, where observed.

Cedar Mountain Formation

Buckhorn Conglomerate Member fluvial sandstones and conglomerates have an average paleoflow direction of 61° (Figure 19). This orientation is roughly parallel to the NE-SW oriented Buckhorn paleovalley that is interpreted to have formed during development of the J-K unconformity across the region (Currie, 1997;1998). The finer-grained and more isolated fluvial-channel sandstones in the overlying Ruby Ranch Member have an average paleoflow orientation of 88°, although measurements across the study area indicate a wide variability in flow directions from NE to SE (Figure 19). This likely reflects a higher sinuosity of Ruby Ranch fluvial systems as they migrated unconfined across the mud-dominated alluvial plain that existed in the region at the time of deposition (Currie, 1998; 2002).

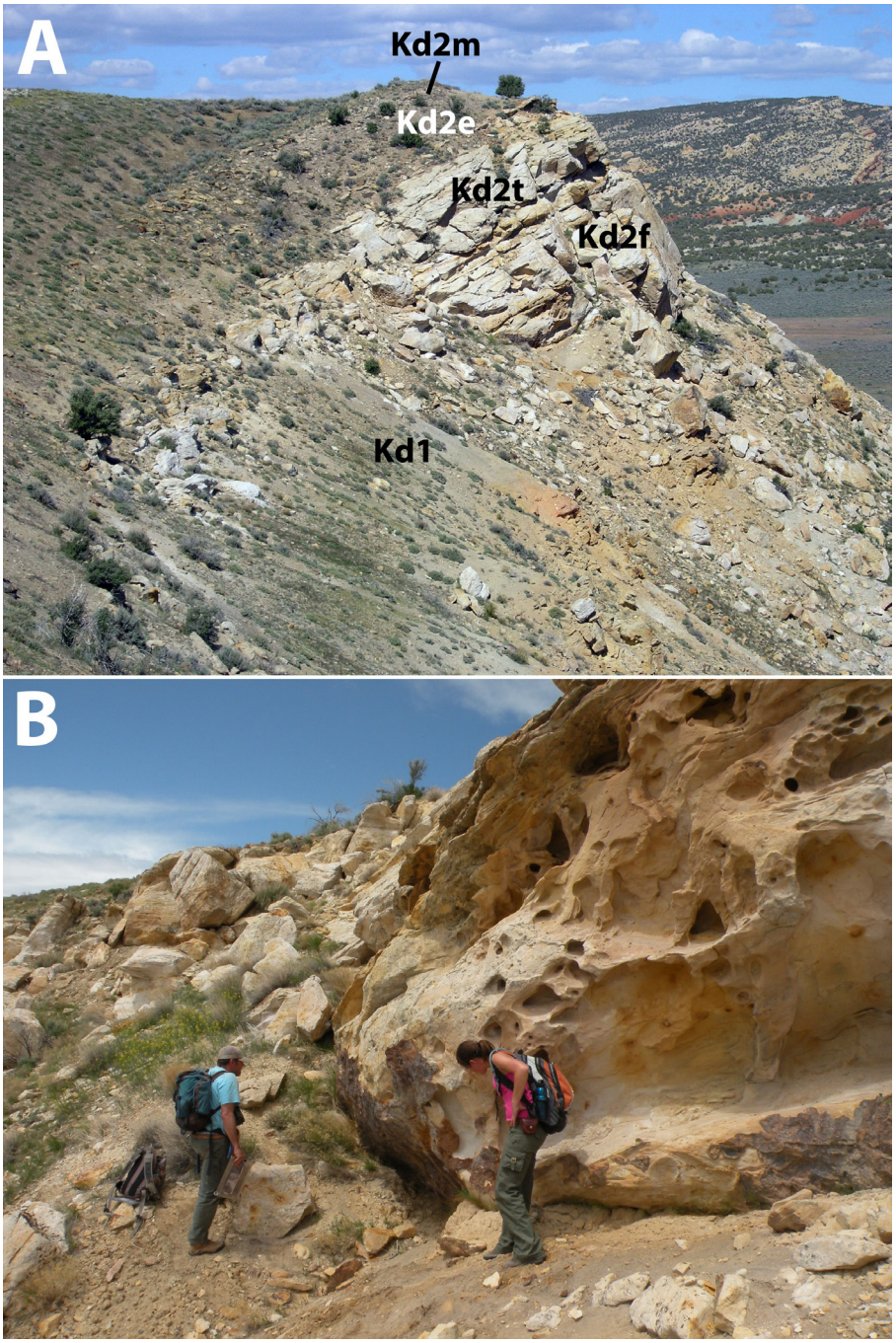

Figure 18. *A) Southern margin of the interpreted Kd2 paleovalley in the Split Mountain Anticline map area near measured section SM 4. Kd1= First Dakota Sequence alluvial/estuarine mudstone; Kd2f= Kd2 fluvial channel sandstone; Kd2t= Upper Kd2 tidal sandstone; Kd2e= Upper Kd2 estuarine mudstone/shale; Kd2m= marine sandstone and conglomerate capping the Kd2 sequence. B) Near-vertical scoured contact between Kd1 mudstone and Kd2 fluvial channel deposits in the same exposure shown in Figure 18A. See Figure 2 and Plate 2 for location.*

Dakota Formation

Kd1 channels in the study area have an average paleoflow direction of 358°. However, this mean orientation is the result of a bimodal distribution of paleoflow directions between the NW and E (Figure 19). While the Kd1 channel sandstones in the study area are intercalated with deposits that display evidence for a tidal influence, it is unclear whether the bimodal distribution of observed paleoflow indicators can be attributed to tidally controlled variations in paleoflow, as the vast majority of the readings were taken from channel sandstones interpreted to have a fluvial origin.

Kd2 channels have a mean paleoflow direction of 349°. The dominantly north directed paleoflow within Kd2 channel forms comes primarily from the fluvial dominated interval, where flow directions ranged from NE to WNW. Ebb tidal current orientations taken from tidally influenced fluvial deposits in the upper part of the sequence indicate a dominantly SE direction of paleoflow.

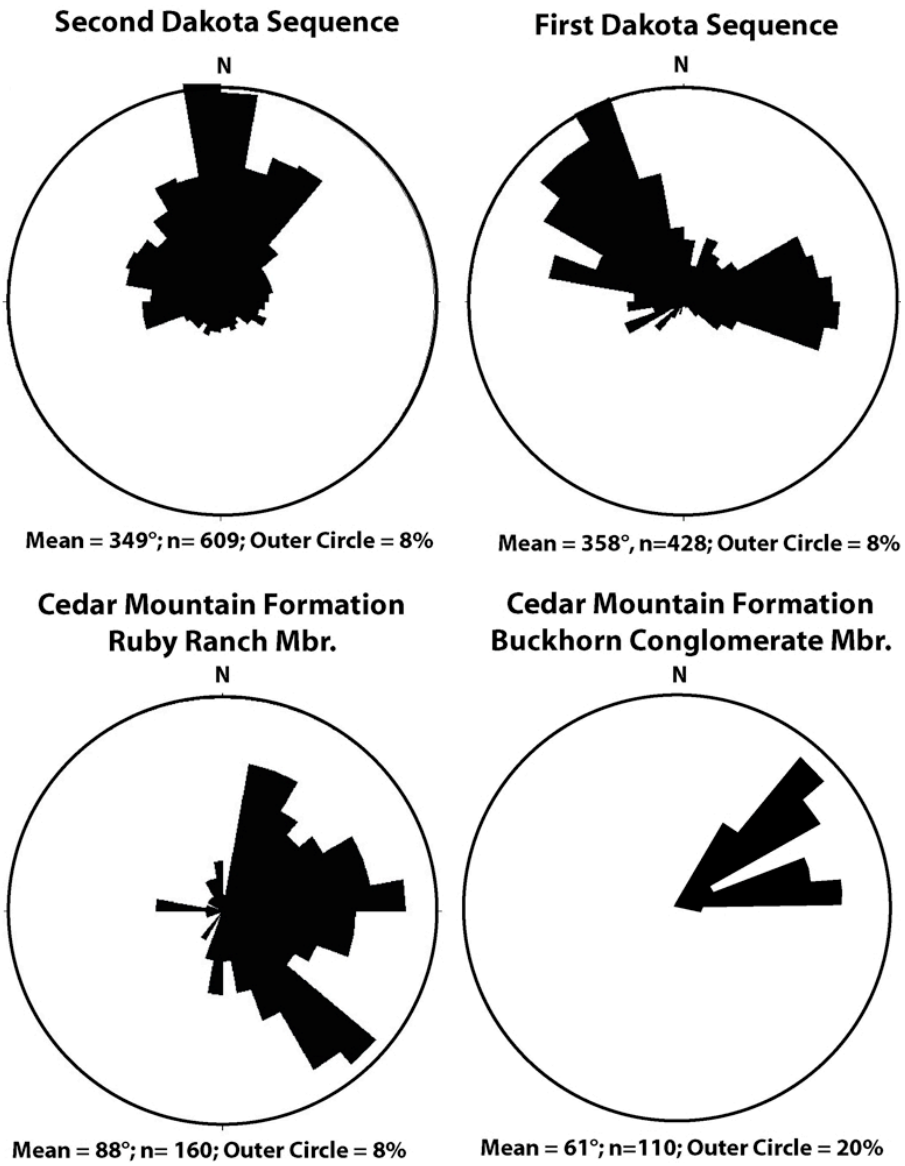

Figure 19. *Rose diagrams of paleoflow directions for the Second Dakota (Kd2), First Dakota (Kd1), and Ruby Ranch and Buckhorn Conglomerate Members of the Cedar Mountain Formation.*

CORRELATION MODEL

This study required the correlation of the following intervals from shallowest to deepest: Mowry Shale, Dakota Formation, Cedar Mountain Formation, Buckhorn Conglomerate Member and Morrison Formation. The correlation model was primarily developed from the model presented in McPherson et al. (2008) and the field work in this study. Lithologic descriptions from other authors, including Molenaar and Cobban (1991), Currie (1998; 2002), Currie et al. (2008a), Pierson (2009), and Sprinkel et al. (2012), were used for additional information.

The correlation area is shown in Figure 20 and purple circles identify the outcrops and wells that were used in this study. Appendix B contains the cross sections used in constructing the correlation envelope shown in Figure 20. Figure 21 is a detailed view of the outcrop with the measured section locations. A scintillometer was used to acquire gamma ray data on all outcrops with the exception of the section measured in 3-4S-21E: Steinaker Canal 1. Outcrop gamma ray logs and their corresponding section descriptions were used as the primary basis for the correlation model. Outcrop gamma ray logs and measured sections through the entire Mowry, Dakota, and Cedar Mountain Formations were acquired at three locations shown in Figure 21. These three outcrop sections are shown below in Figure 22.

The Dakota Formation was used as the correlation datum for the project. The top of the Mowry Shale is an excellent datum for the subsurface but full gamma-ray logs are difficult to acquire in the outcrop due to erosion, deep weathering or covering by vegetation and colluvium. It was also difficult to acquire gamma-ray logs through the Ruby Ranch Member mudstones of the Cedar Mountain Formation due to deep weathering or poor exposures.

The thickness of the CMD interval is approximately 300 ft over most of the study area but increases to approximately 350 ft in

the extreme northwest of the study area and where the Buckhorn Conglomerate is present in the eastern part of the study area. In the following discussion, the log character of the Mowry Shale will be described first as all subsurface wells were originally hung on this datum for correlation. The correlation model for the CMD interval will be described from the top down. This inverted description is used as it more closely coincides with how these rocks are correlated on well logs.

Mowry Shale

The lower Cenomanian Mowry Shale is marine with a consistent log pattern of stacked coarsening-upward sequences and is overlain by the Tununk Shale Member of the Mancos Group.

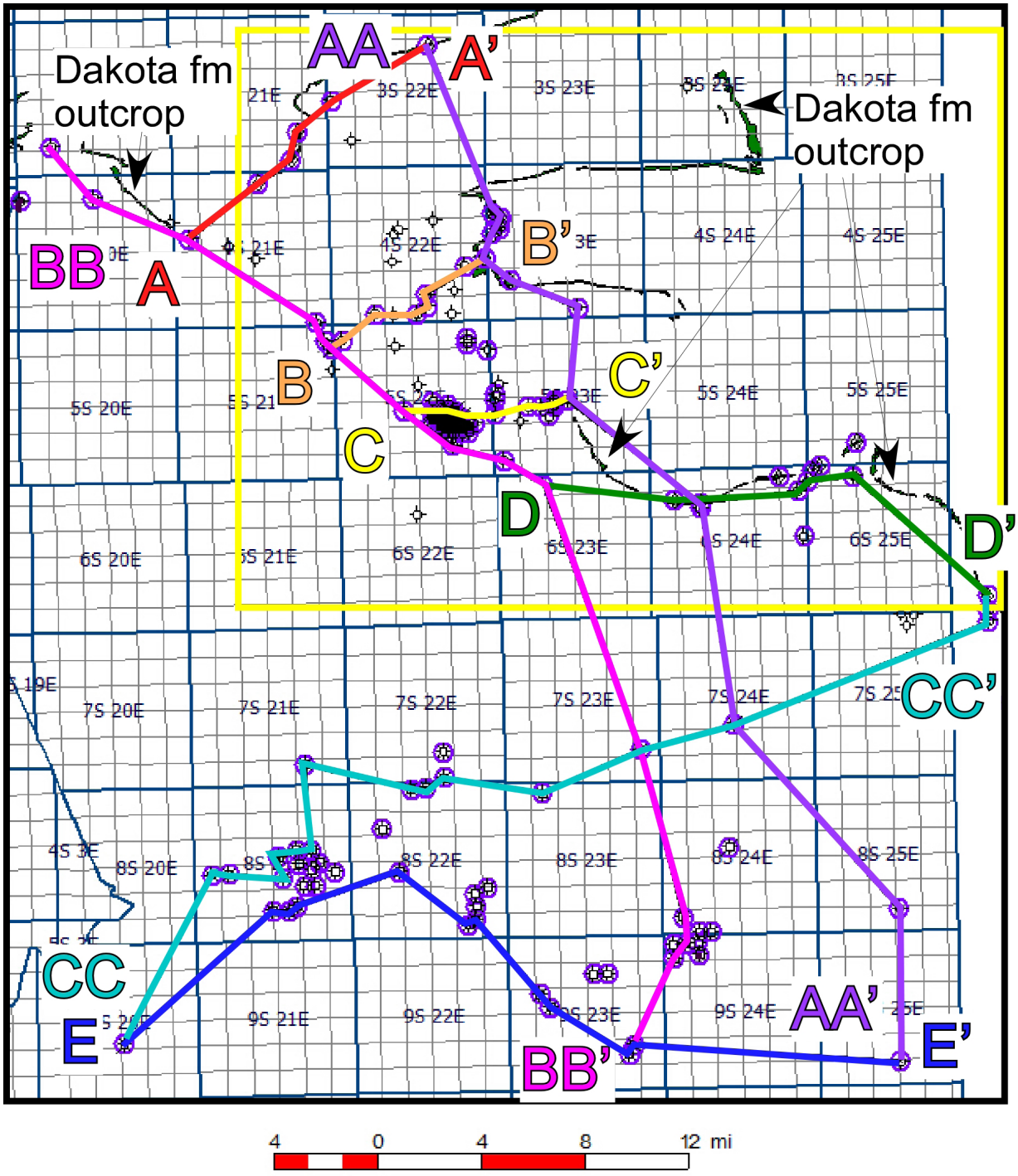

Figure 20. *Map showing lines of stratigraphic correlation (correlation envelope) in the study area. Purple circles identify the wells and outcrops that were correlated as part of this study. The colored lines show the correlation envelope that was used as the correlation basis. The yellow box is detailed in Figure 21. The cross sections are included in Appendix B.*

The top of the Mowry Shale coincides with the middle Turonian unconformity (Molenaar and Cobban, 1991). In the southern part of the study area, upward-coarsening shoreface deposits are well-developed and evince blocky gamma ray patterns in their upper parts. The Mowry varies in thickness from 70 ft in the northeastern part of the study area to 160 ft in the southern part where the shorefaces are well-developed (Appendix C: Mowry Shale). In Ashley Valley Field, 5S-22E, normal faults may shorten the section by up to 20 ft.

We define the Mowry Shale top as the gamma ray peak above an overall coarsening-upward section near the base of the lower Mancos Group. Figures 22 and 23 show this pattern in outcrop and subsurface gamma rays. In the subsurface, the Mowry Shale top is placed in the center of a lower lobe of resistivity with a W-shape that coincides with a high gamma ray peak. The high gamma ray peak is representative of a marine flooding surface that encroached on the middle Turonian unconformity.

Dakota Formation

The Dakota Formation is a series of inter-fingering fluvial, estuarine, and marine deposits in the study area. The thickness varies from 60 to 190 ft (Appendix C: Dakota Formation). Commonly, a basal fluvial interval is incised into the underlying Cedar Mountain Formation and is overlain by estuarine and/or swamp deposits (Kd1). This is in turn incised by upper Dakota Formation (Kd2) fluvial systems that fine up and are frequently overlain by estuarine mudstone and/or sandstone. The very top of the Dakota Formation is marked by transgressive-lag sandstone. The log signature for the Dakota Formation is quite variable as shown in the cross sections contained in Appendix B.

The Dakota Formation can be subdivided into an upper and lower Dakota Formation, Kd2 and Kd1, respectively as defined earlier in this report. This division is based on palynology and lateral relationships that can be mapped in the field.

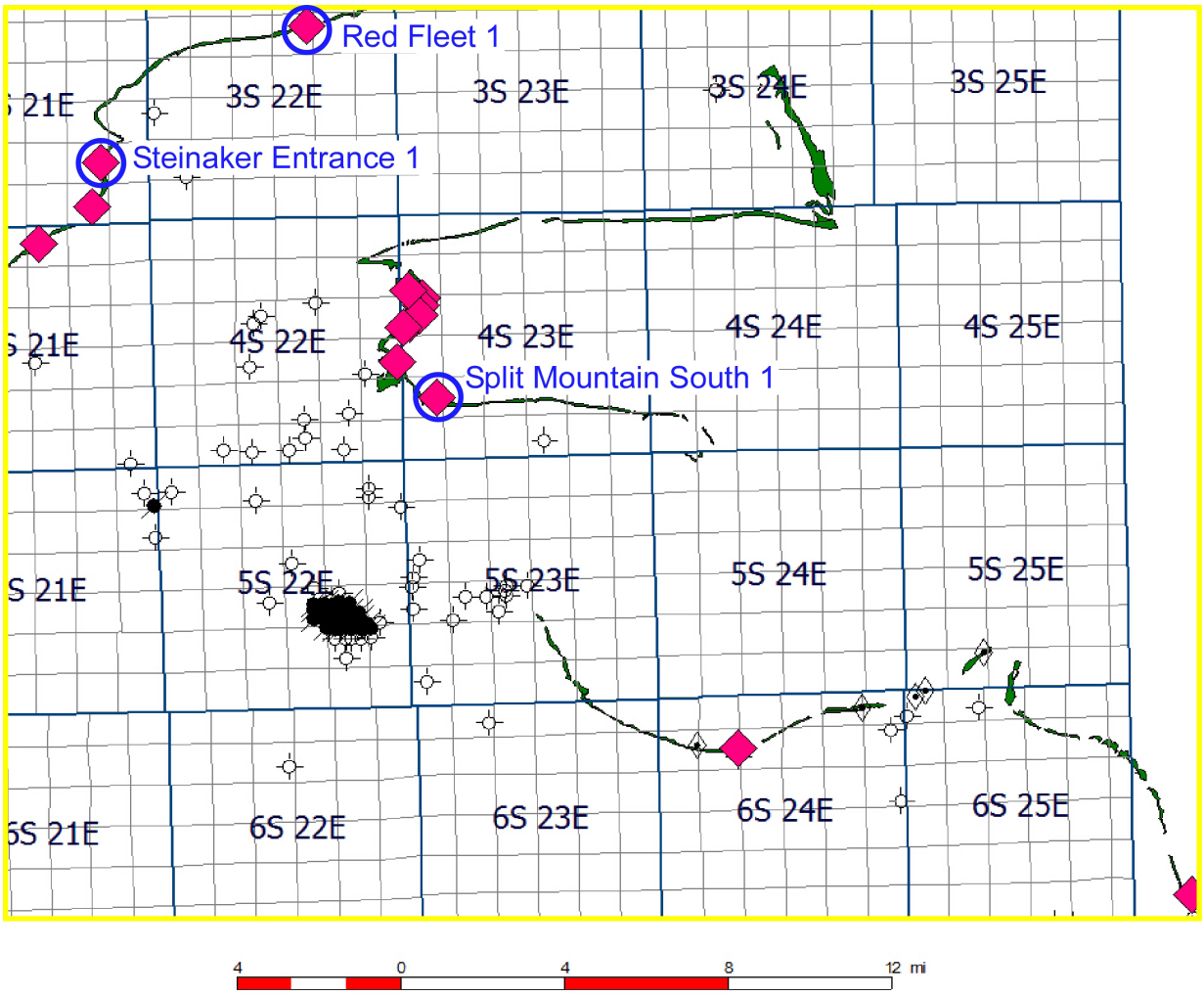

Figure 21. *Detail map (area bounded in yellow in preceding figure) of outcrop locations where measured sections +/- gamma ray data were acquired. The Dakota Formation outcrop is shown in green. The 3 outcrop sections marked with blue circles are the measured sections (with gamma rays) of the upper Morrison Formation to lower Frontier Formation that are shown in Figure 22. All outcrop sections are included in cross sections in Appendix B.*

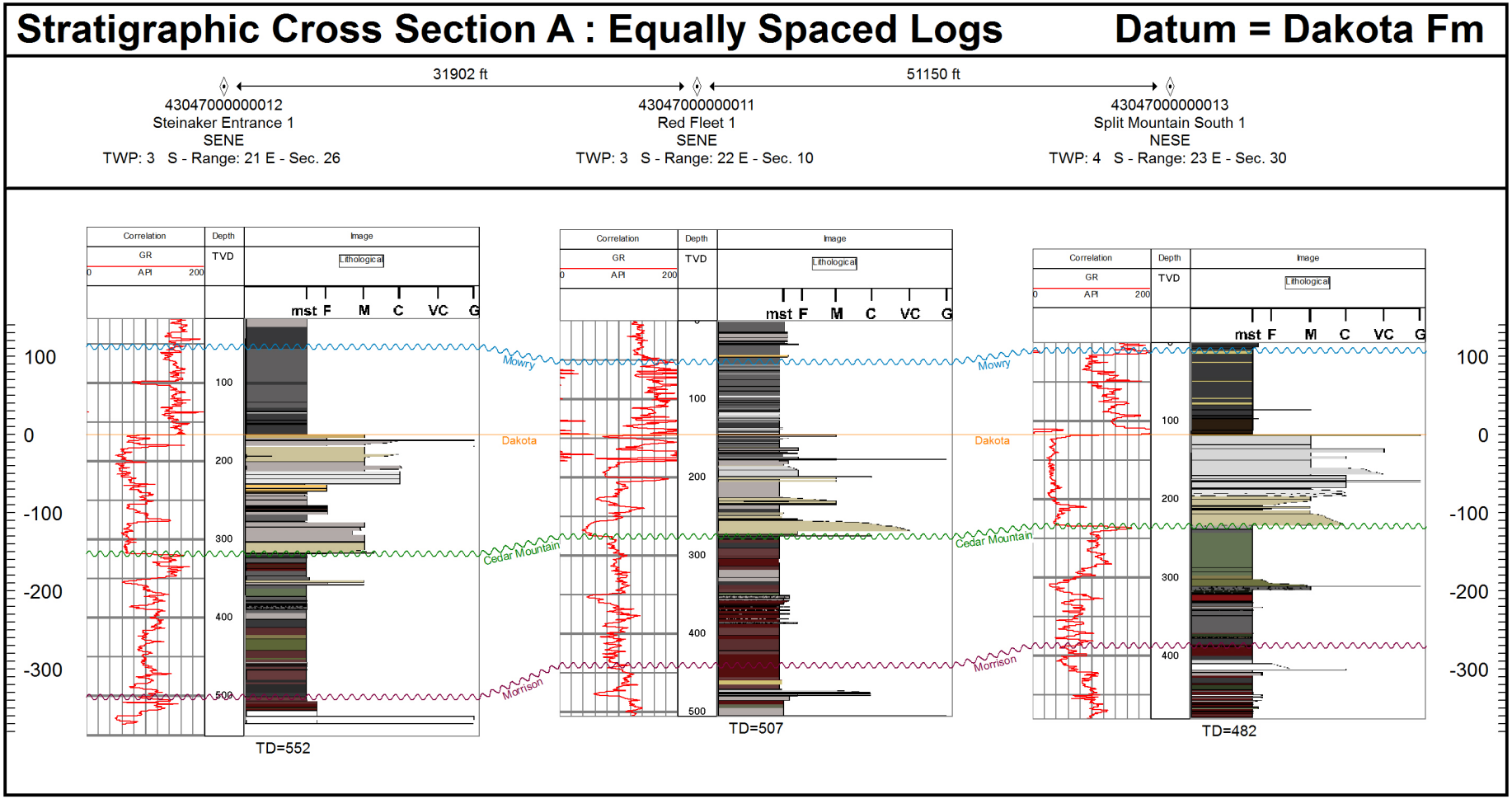

Figure 22. *Measured sections and gamma ray logs for three outcrops where the entire interval from top of Mowry Shale through top of Morrison Formation was described. Locations are shown on Figure 21. The colors on the measured sections represent the colors of the lithologies in the outcrop. Stratigraphic units correlated in this study are the Mowry, Dakota, Cedar Mountain, and Morrison Formations. Thickness is in feet; datum is the top Dakota Formation.*

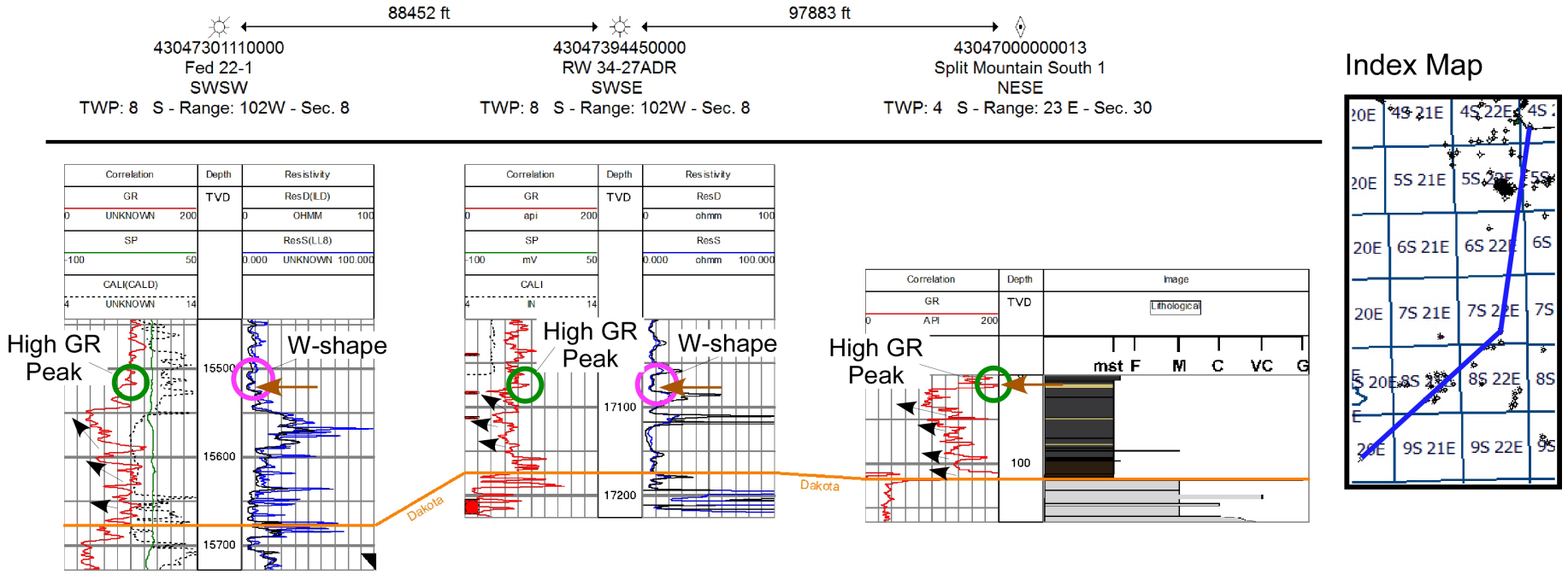

Figure 23. *Criteria for correlating the top of the Mowry Shale in the study area. The pick is indicated by the brown arrow and coincides with a high gamma ray peak above a series of coarsening-upward cycles. This high gamma ray peak is coincident with low resistivity in the lower lobe of a W-shape on the resistivity curves in the subsurface.*

However, we are unable to confidently carry these subdivisions into the subsurface, especially in areas with shale-on-shale contacts. Marine sub-units, such as Kd1 Estuarine sandstone can be correlated and mapped as shown in Plates 4 and 5.

Criteria for picking the top of the Dakota Formation are similar to what were described McPherson et al. (2006, 2008). In the southern Uinta Basin the Mowry Shale is only present in the far eastern reaches of the basin due to erosion represented by the middle Turonian unconformity or non-deposition. In the northern Uinta Basin, the Mowry Shale is present across the entire area. This has resulted in a slight modification of the pick.

Near the top of CMD-interval outcrops in the study area, a gravelly wave-rippled interval is pervasive across the area (Figure 16) and often forms the dip-slope on the outcrops. It is an excellent marker bed although too thin for resolution on the common subsurface logs in the area. Frequently, the gravelly wave-rippled bed is overlain by interbedded dark gray shale, fine- to coarse-grained sandstone and granule-pebble conglomerate (Figure 16). The uppermost sandstones and conglomerates in the CMD interval contain hummocky, and trough cross-stratification, as well as both unidirectional and oscillatory ripples. In places they are highly bioturbated. In several of our measured outcrop sections, these coarse-grained transgressive marine deposits directly overlie Kd2 fluvial channel sandstones (e.g., Steinaker Entrance, RT 191 Road Cut, State Line sections, Plate 1). For this reason, we place the top of the Dakota Formation at the top of the thin transgressive marine sandstone/conglomerate that is immediately overlain by the dark gray/black shale of the Mowry Shale. In many of our measured outcrop sections, the top of the measured section coincides with the top of the Dakota Formation.

The gamma ray and/or high-resolution (shallow) resistivity curves were used to correlate the top of the Dakota Formation in the subsurface. SP curves were useful in older wells. Figure 24 shows the contact in outcrop measured sections, and boreholes with old and modern well logs. The old well (Stewart Fee 1) is also an example of a well where the lag and overlying marine sandstone probably lie directly on thicker Dakota Formation sandstone, as occurs in the Split Mountain South 1 outcrop (30-4S-23E) shown in Figure 22.

We define the top of the Dakota Formation as the inflection point on the gamma ray curve above a thin sandstone that coincides with a change from low Mowry Shale resistivity to higher resistivity in the Dakota Formation. In wells where the thin sand and gravel beds lie directly on a thick sandstone, the top of the Dakota Formation is picked at the top of the sandstone. The contact commonly equates to the occurrence of an SP response in the underlying Dakota Formation.

Cedar Mountain Formation

In the study area, Ruby Ranch and Buckhorn Conglomerate Members make up the Cedar Mountain Formation. Where the Buckhorn Conglomerate is absent, the Ruby Ranch Member lies directly on the Morrison Formation. The Cedar Mountain Formation ranges from ~110 to 230 ft in the study area (Appendix C: Cedar Mountain Formation). The model for correlating the top of the Cedar Mountain remains unchanged from McPherson et al. (2006; 2008).

Ruby Ranch Member

The Ruby Ranch Member of the Cedar Mountain Formation consists of interbedded mudstones and sandstones deposited in fluvial channel and overbank environments. It ranges from 75 to 230 ft and thickens to the west and northwest across the study area (Appendix C: Ruby Ranch Member). The Ruby Ranch Member is characterized by pedogenic-carbonate nodules and calcretes.

Overall, the Ruby Ranch Member exhibits a fining-upward gamma ray signature. The upper part of the Ruby Ranch Member is marked by increased smectite towards the Dakota Formation contact, which accounts for the apparent fining-upward signature. Carbonate also diminishes towards the contact between the Dakota Formation and Ruby Ranch Member. Organic-rich fluids that were expelled from the carbonaceous-rich intervals of the Dakota Formation are likely responsible for this carbonate dissolution and smectitic enrichment (Currie, 2002).

The top of the Cedar Mountain Formation is picked at a high gamma ray peak at the top of a fining-upward sequence where the contact is shale on shale (Figure 25). Relatively high gamma ray readings occurring above this peak likely represent Kd1 estuarine/alluvial mudstones/shales. Where basal Kd1 channel sandstones are incised into the underlying Ruby Ranch Member, the base of the channel is typically marked by a very high gamma ray peak, indicative of smectitic enrichment (Figure 26) at the contact.

Typically, the main body of the Ruby Ranch Member evinces a serrated profile on both gamma ray and resistivity logs as signified by the vertical blue arrow in Figures 25 and 26. This is caused by the occurrence of multiple discrete paleosols, accompanied by numerous calcrete nodules low in the interval, which are interbedded with fluvial sandstone up to 20 ft thick and overbank siltstones.

Buckhorn Conglomerate

The Buckhorn Conglomerate Member of the Cedar Mountain Formation crops out along the southern side of the Split Mountain anticline, which coincides with the northeast edge of the mapped area shown in Appendix C: Buckhorn Con-

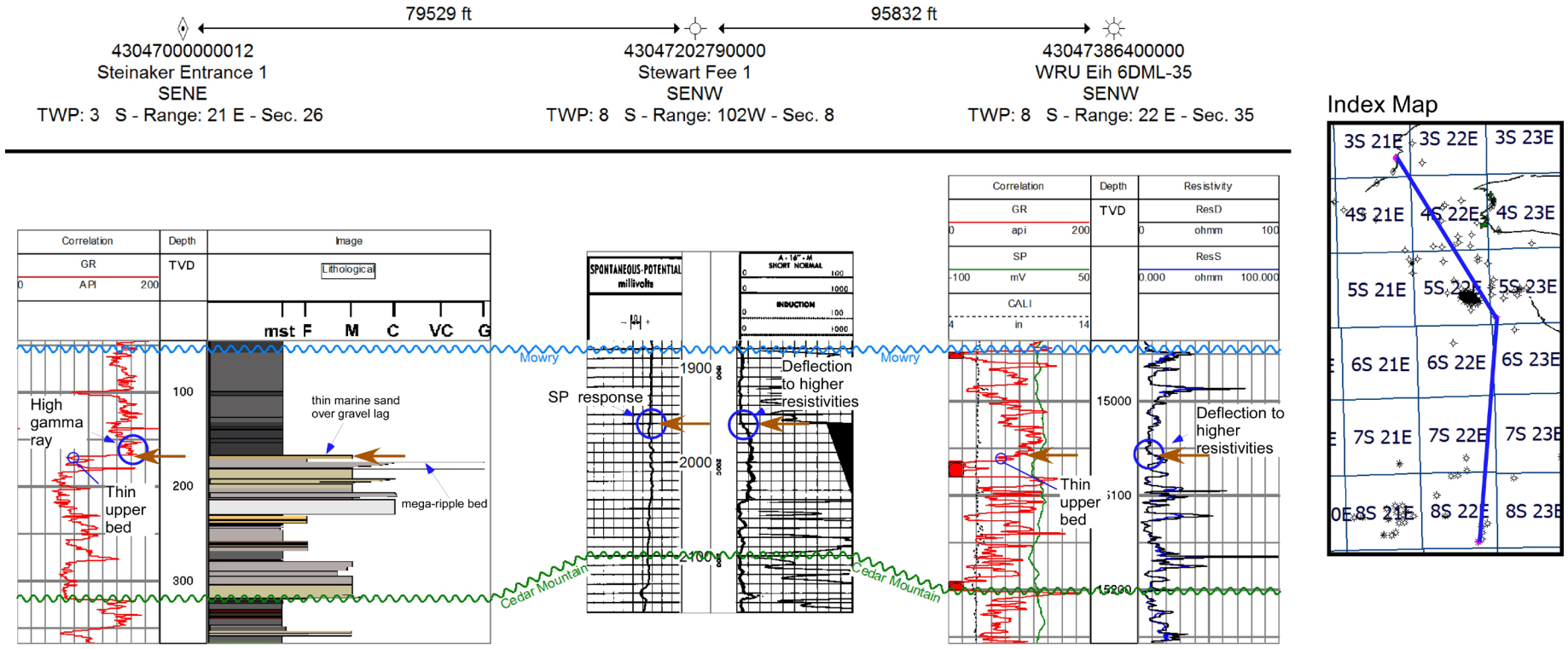

Figure 24. *Outcrop section and subsurface well logs showing criteria for picking the top of the Dakota Formation. The pick is indicated by the brown arrow and coincides with the top of a thin sandstone that is overlain by an interval with high gamma ray, low resistivity and no SP response. Occasionally, the top of the Dakota Formation will coincide with the first thick sandstone with increased resistivity and SP deflection as compared to the overlying Mowry Shale. This is shown in the Stewart Fee 1 well. The outcrop and the WRU Eih 6DML-35 show the more typical signature of the top of the Dakota Formation.*

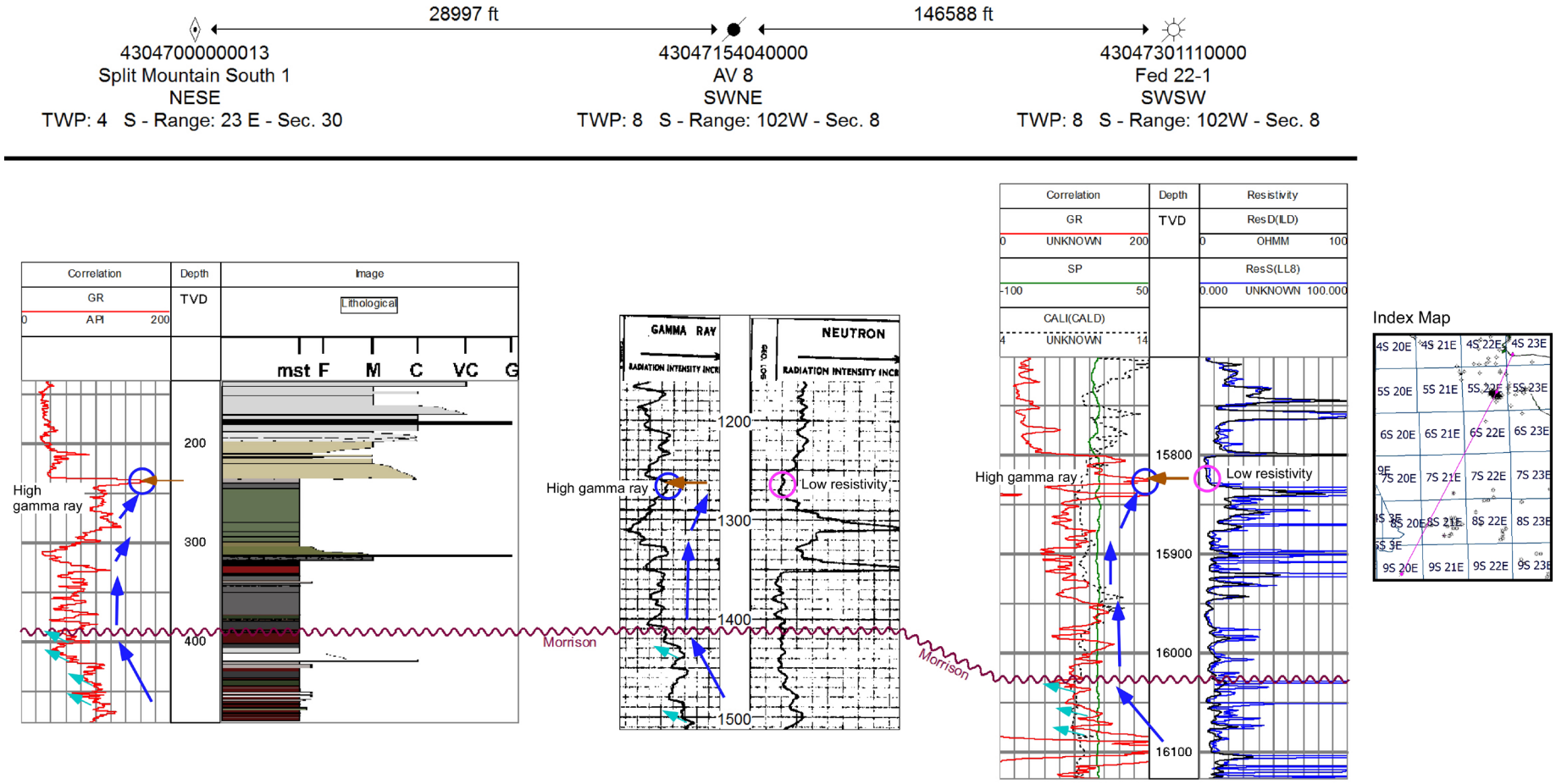

Figure 25. *Outcrop section and subsurface well logs showing criteria for picking the top of the Ruby Ranch Member of the Cedar Mountain Formation. The pick is indicated by the brown arrow and coincides with a high gamma ray peak with coincident low resistivity. Where the Ruby Ranch Member directly overlies the Morrison Formation, the gamma ray commonly evinces an overall C-shape from the upper part of the Morrison Formation to the top of the Ruby Ranch Member. The center serrated section of the gamma ray (indicated by the vertical blue arrow) represents the main body of the Ruby Ranch Member. The gamma ray then deflects to higher values as a result of smectitic enrichment. The upper Morrison Formation displays an apparent coarsening-upwards pattern as a result of calcrete overprinting and leaching of paleosols. The teal arrows indicate stacking of individual paleosol cycles with apparent coarsening-upward profiles.*

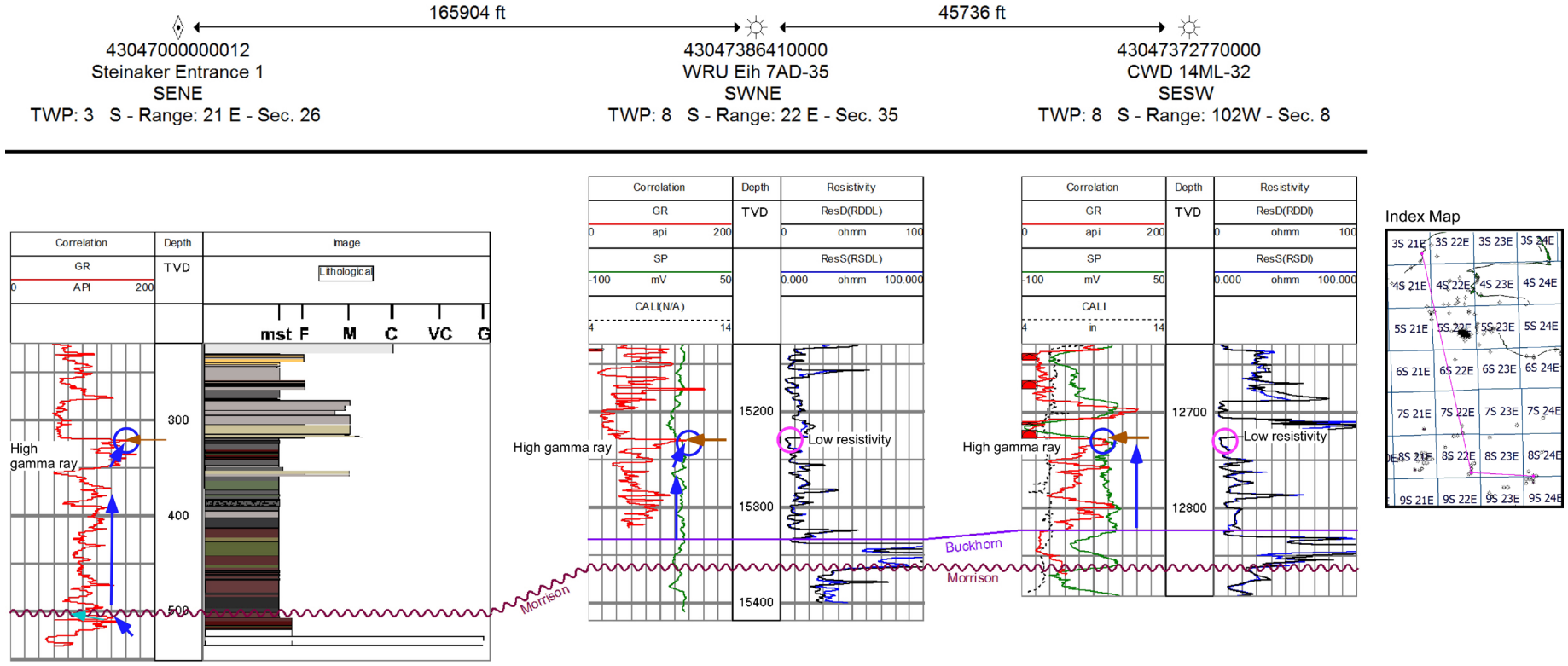

Figure 26. *Outcrop section and subsurface well logs showing additional examples for picking the top of the Ruby Ranch Member of the Cedar Mountain Formation when it lies below Kd1 channels. The pick is indicated by the brown arrow and coincides with a high gamma ray peak with coincident low resistivity. Where the Ruby Ranch Member directly overlies the Morrison Formation, the gamma ray commonly evinces an overall C-shape from the upper part of the Morrison Formation to the top of the Ruby Ranch Member. The center serrated section of the gamma ray (indicated by the vertical blue arrow) represents the main body of the Ruby Ranch Member. This cross section also shows the contact between the Ruby Ranch and Buckhorn Members of the Cedar Mountain Formation.*

glomerate Member. It varies in thickness from 0 to ~100 ft in the study area. The log pattern is consistent with what was observed in McPherson et al. (2006; 2008). Figure 27 shows the Buckhorn Conglomerate log signature in both the subsurface and outcrop. The gamma ray logs display a blocky sandstone profile with a thin mudstone interval in the middle and a fining-upward profile at the very top. This corresponds to an overall high resistivity pattern. In outcrop, the top of the fining-upward interval may be associated with a basal Ruby Ranch Member calcrete horizon, which overprints uppermost Buckhorn lithologies. The top of the Buckhorn Conglomerate is defined at the top of a fining-upward interval with coincident inflections on the gamma ray and resistivity logs. The base of the Buckhorn Conglomerate is pronounced on the gamma ray log and frequently on the resistivity log also. The base of the Buckhorn Conglomerate rests on the Morrison Formation.

Basal Contact with the Morrison Formation

Field observations confirmed the correlation model of McPherson et al. (2006; 2008) for the top of the Morrison Formation. The outcrop gamma ray logs show a subtle, but consistent C-shape from the upper-most part of the Morrison Formation to the Ruby Ranch Member contact with the Dakota Formation. As Figure 25 illustrates, the overall pattern at the top of the Morrison Formation is an apparent coarsening-upward and the pattern of the Ruby Ranch Member is serrated to fining-upward. The base of the Cedar Mountain Formation is put at the turn-around from the apparent coarsening-upward to the serrated log pattern in the C-shape where the Buckhorn Conglomerate is not present. Where the Buckhorn Conglomerate is present, the base of the Cedar Mountain Formation is put at the base of the conglomerate.

A regionally-extensive paleosol or weathered horizon occurs at the top of the Morrison Formation in outcrops across the Colorado Plateau (Currie, 1997; Demko et al., 2004). The very top of this paleosol is leached of clays and indurated with calcium carbonate from the overlying Ruby Ranch Member, thereby causing an apparent coarsening-upward trend on the gamma ray. In the subsurface, this gamma ray profile is accompanied by a slight increase in resistivity on the high-resolution curve with no deflection of the SP (Figure 28).

WELL CORRELATION

The correlation model described above was used to correlate the wells in the study area. The majority of wells were correlated with raster logs downloaded from the Utah DOGM website. Nearly all digital logs were supplied by QEP Resources. Outcrop gamma ray logs were acquired in the field with a scintillometer.

A correlation envelope was developed by constructing eight cross sections, which are contained in Appendix B. The cross section locations are shown in Figure 20. Wells interior to the correlation envelope were then correlated. A few wells were faulted through the interval Mowry Shale to Morrison Formation but offsets were less than 20 ft.

Tops may be off in old wells with E-logs and old neutron logs. Bed resolution may be insufficient to define the subtle patterns that we looked for. These wells were compared with offset wells to minimize misinterpretation. An uncertainty is also introduced in many older wells where the logs are off depth from each other or the scanned image was extremely skewed. Usually, the gamma ray log was used to pick tops. However, in some instances, the gamma ray quality was very poor and the resistivity log was used for the correlation. In some wells, available digital logs did not cover the bottom of the well and tops were picked on the Cement Bond Log (CBL) raster image obtained on the Utah DOGM website.

Correlations were quality checked by constructing isopach and structure contour maps of each horizon. Quality control maps were constructed in Geographix using the following parameters: gridding algorithm = "Minimum curvature", forced data honoring was implemented, "Max iterations" = 25, convergence = 0.1 and "simplified defaults" was selected for grid spacing. A geologic bias with a magnitude of 1.25 was introduced in intervals with paleocurrent data. No hand editing of contours was performed except for the isopach of the Buckhorn Conglomerate where the grid was edited to define the pinch outs of the fluvial system. Isopach maps included in Appendix C are for the Mowry Shale, Dakota Formation, Cedar Mountain Formation, Ruby Ranch Member and Buckhorn Conglomerate Member. Structure contour maps for the Mowry Shale, Dakota Formation, Cedar Mountain Formation and Morrison Formation are also included in the Appendix C. Faults were not included in the structure maps as these maps were only used for quality control purposes. The measured depth tops for each correlated well are contained in Appendix D.

CMD PRODUCTION

The lower Cretaceous CMD is gas productive in ~40 deep wells in the northern Natural Buttes area (Fig. 29). These wells typically contain completed zones over a several thousand-ft interval that ranges from the Eocene-Paleocene Wasatch Formation through the Lower Cretaceous CMD. Production is commingled in these wells. Only one well is a CMD-only completion (Glen Bench 9D-27, API 43047349560000, NE SE 27-8S-21E), the only red bubble in Figure 29. All wells were drilled, completed, and are currently operated by QEP Energy.

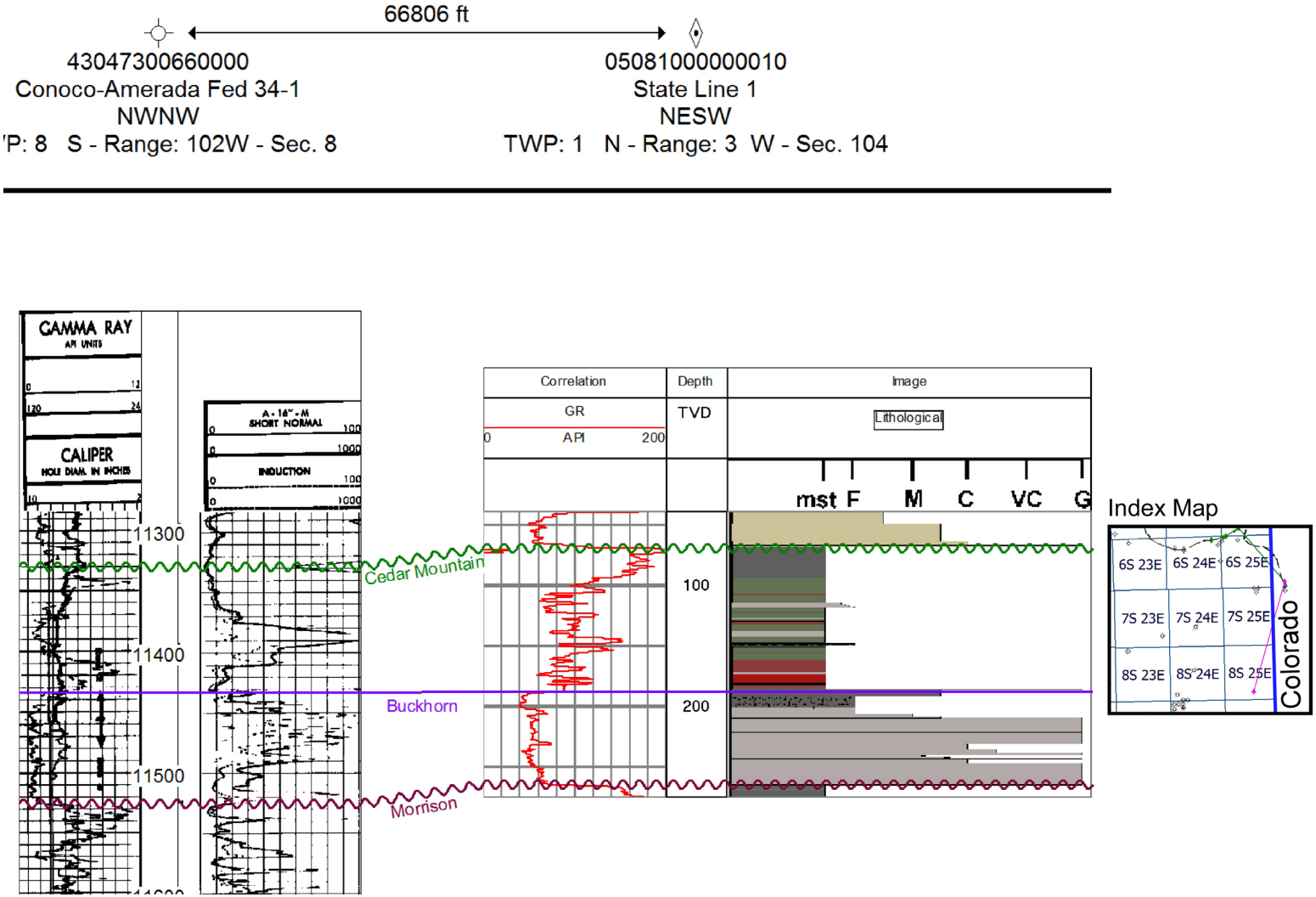

Figure 27. *Subsurface and outcrop logs showing Buckhorn Conglomerate Member log response. The gamma ray is low and blocky and resistivity is usually high. The interval generally fines upward at the very top. Thin mudstones are indicated by higher gamma ray and low resistivity. The basal contact is sharp.*

Production Allocation

QEP reported Fluid Entry Tests (FETs) or assigned allocations based on offset wells' FETs, and reported these numbers to the Utah DOGM. Table 1 is a compilation of these data and includes cumulative gas (and water where possible) production for the CMD. This table lists all wells where QEP included the "Kd" (Dakota Formation) as a producing horizon.

For some wells, QEP reported allocated production by gross stratigraphic interval including Wasatch, Mesaverde, Mancos, Mancos B, Frontier, Mowry and Dakota until 1 March 2009. Thereafter, comingled production was reported for the entire perforated interval as it had been for other wells throughout the duration of their production history. Where the production was initially reported by stratigraphic interval, the assigned gas production was usually based on the allocations that were reported to the Utah DOGM. Exceptions are the GB 8D-20 in SENE 20-8S-22E, API 43047376650000, and the RW 34-27ADR in SWSE of 27-7S-22E, API 43047363510000. Both wells had FETs run where the CMD gas production was 0% yet gas production was reported to the Utah DOGM for the Kd interval. In this report, the cumulative gas production was determined by using all FET data that were supplied to the Utah DOGM. For example, the GB 8D-20 referenced above had 3 allocations (Table 1) submitted to the Utah DOGM: June 2007 – 23.5% of the gas assigned to the Kd based on a FET, October 2007 – 0% of the gas assigned to the Kd based on a FET and June 2008 – 23% of the gas assigned to the Kd based on offset wells. These allocations were applied to the reported monthly productions for the time periods of May 2007 (completion) to October 2007(23.5%), October 2007 to June 2008 (0%) and June 2008 to September 2008 (23%). All of the cumulative gas production data compiled for this study were calculated in a similar manner.

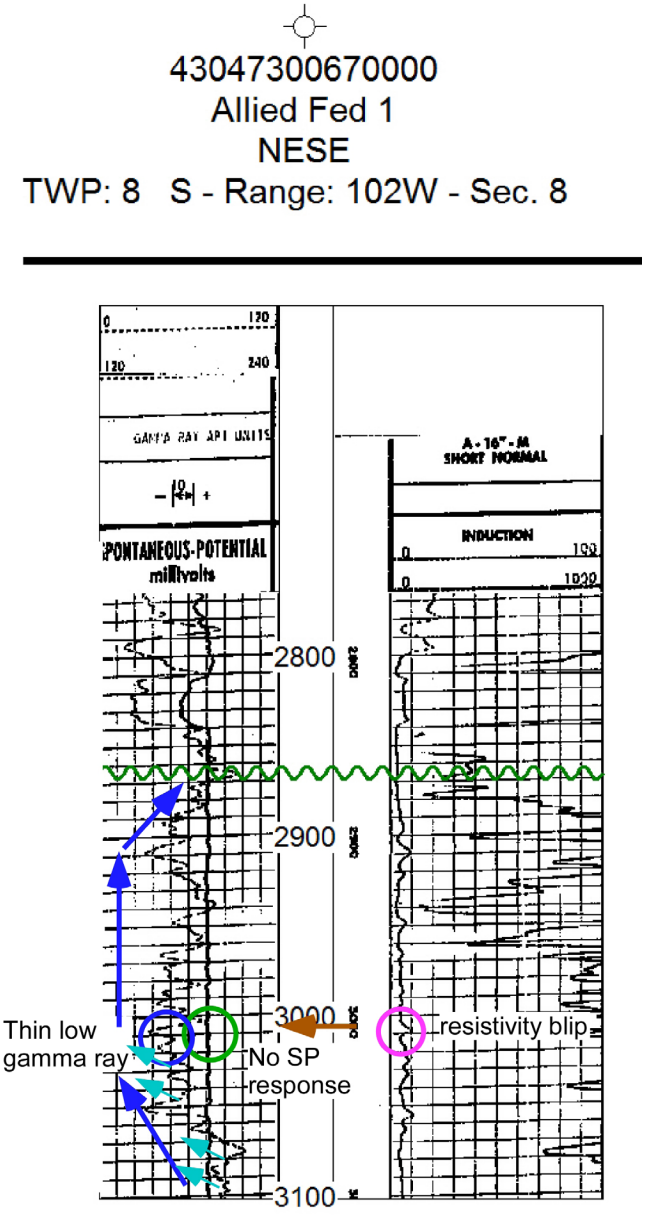

Figure 28. *Well log showing criteria for picking the top of the Morrison Formation where the Buckhorn Conglomerate is not present. The uppermost thin apparent coarsening-upward bed at the top of a cycle of stacked apparent coarsening-upward beds coincident with no SP deflection and a resistivity blip is chosen as the contact between the Cedar Mountain (Ruby Ranch Member) and Morrison Formations (brown arrow).*

In most instances, QEP's reported water production appears to have been calculated by applying the gas allocation to the water production. In this study, cumulative water production was only derived for wells with actual FETs. Most FETs indicated minor water production from the CMD interval. An exception is the WV 13AD-8 in SWSW 8-8S-22E, with an FET-based water allocation of 43%. The FET analysis states that this reported water production may be "too high or non-existent." Therefore, in Table 1 we do not report a water allocation for this well.

QEP's reported oil production appears to have been assigned to one zone or it is equally divided across all zones. Therefore cumulative oil production was not calculated for CMD producers. Oil production from the CMD is expected to be insignificant, as shown by the cumulative oil production of the one CMD-only completion: 632 Bbls in GB 9D-27 in NESE 27-8S-21E.

In Table 1, the cells highlighted in green represent FETs that were in the Utah DOGM on-line well files. The other allocations are based upon offset production logs as reported by QEP. As Table 1 shows, most of the reported production is based on offset production logs of which there are few. Only two wells had multiple FETs reported to the DOGM: NBE 10D-26 in NWSE of 26-9S-23E, API 43047366200000, and GB 8D-20 in SENE 20-8S-22E, API 43047376650000. The CMD gas contribution varied from 0% on 2-2-07 to 57% on 8-24-07 for the NBE 10D-26, and from 23.5% on 6-21-07 to 0% on 10-15-07 for the GB 8D-20. The production behavior of these two wells and the lack of actual FETs for other CMD completions indicate that allocated production in the CMD wells is probably baseless and not useful for any analysis.

Table 1. *List of wells that were reported to the Utah DOGM as producing from the "Kd" (Dakota Formation). Cells highlighted in green represent actual fluid entry tests. All other allocations were purportedly based on "offset well tests".*

Well ID (API Number)	Well Name	Completion Date	Producing Formation*	Cumulative Oil (BBL)	Cumulative Gas (MCF)	Cumulative Water (BBL)	Production Allocations								Cumulative Kd gas (MCF)	Cumulative Kd water (BBL)
							Date	% Gas	% Water	Date	% Gas	% Water	Date	% Gas		
43047349020000	WVX 11D-22-8-21	10/27/07	Kmv + Km + Kf + Kd	4,722	1,171,612	100,196		NONE REPORTED								
43047349560000	GB 9D-27-8-21	04/16/07	Kd	632	2,750,969	8,769		NA							2,750,969	8,769
43047349570000	GB 1D-27-8-21	09/01/06	Kmv + Km + Kd	1,492	860,850	88,219	05/18/07	36							309,906	0
43047362600000	GB 16D-28-8-21	03/10/06	Kmv + Km + Kd	4,131	1,073,458	107,175	04/01/06	7	40						75,142	42870
43047363510000	RW 34-34 AD	03/25/08	Tw + Kmv + Km + Kf + Kd	3,893	301,919	51,299	04/20/09	20	water allocation = gas allocation						61,656	0
43047366200000	NBE 10D-26-9-23	05/22/07	Kme + Km + Kf + Kd	5,079	481,904	137,770	02/07/07	0	0	08/24/07	57	4			2,315	4061
43047369820000	RW 04-25B	08/21/08	Kmv + Km + Kf + Kd /Tw + Kmv + Km + Kf + Kd	8,157	613,555	114,644	03/12/09	10	water allocation = gas allocation						35,607	0
43047372380000	NBZ 8D-31-8-24	02/01/08	Tw + Kmv + Km + Kf + Kd	10,724	502,020	85,136		NONE REPORTED								
43047372770000	CWD 14ML-32-8-24	08/02/07	Tw + Kmv + Km + Kf + Kd	12,781	871,298	43,394	04/13/09	12							104,556	0
43047372780000	CWD 16D-32-8-24	05/26/08	Tw + Kmv + Km + Kf + Kd	12,930	271,564	44,652	04/13/09	78							211,820	0
43047373100000	RWS 14D-5-9-24	06/23/08	Tw + Kmv + Km + Kf + Kd	2,820	254,691	42,716	06/24/08	10							25,469	0
43047373470000	CWD 10D-32-8-24	03/11/08	Tw + Kmv + Km + Kf + Kd	14,047	597,826	53,221	03/13/08	15		06/13/08	15				89,674	0
43047373500000	RWS 6D-5-9-24	06/30/07	Tw + Kmv + Km + Kf + Kd	4,900	261,131	67,399	Kd Excluded w/ CIBP during completion								NA	0
43047373520000	RWS 8D-6-9-24	02/23/07	Tw + Kmv + Km + Kf + Kd	8,985	832,889	97,283	05/10/07	0		04/13/09	0				0	0
43047374130000	RWS 6D-6-9-24	06/05/07	Tw + Kmv + Km + Kf + Kd	4,489	373,035	80,261	04/13/09	10							163,172	0
43047374140000	RWS 14D-6-9-24	12/01/07	Tw + Kmv + Km + Kf + Kd	2,815	104,616	46,090	Kd Excluded w/ CIBP 2-25-08								NA	0
43047376650000	GB 8D-20-8-22	05/30/07	Tw + Kmv + Km + Kf + Kd	11,542	603,043	117,309	06/21/07	23.5	0	10/25/07	0	0	06/13/08	23	105,783	0
43047376710000	BZ 10D-16-8-24	08/30/07	Tw + Kmv + Km + Kf + Kd	5,679	77,346	37,649	04/20/09	10							7,735	0
43047380490000	WV 11AD-14-8-21	06/05/08	Tw + Kmv + Km + Kf + Kd	4,594	537,636	58,311	09/12/08	17	0	03/12/09	10				74,285	0
43047382670000	GH 7D-19-8-21	09/18/08	Tw + Kmv + Km + Kf + Kd	3,783	596,254	45,840	03/12/09	20							119,478	0
43047386360000	WRU EIH 4AD-25-8-22	04/15/08	Tw + Kmv + Km + Kf + Kd	5,667	340,305	43,338	06/13/08	10	water allocation = gas allocation						35,243	0
43047386370000	WRU EIH 7AD-26-8-22	03/18/08	Tw + Kmv + Km + Kf + Kd	7,139	530,291	32,044	06/13/08	20	water allocation = gas allocation						106,394	0
43047386400000	WRU EIH 6DD-35-8-22	03/07/08	Tw + Kmv + Km + Kf + Kd	9,835	925,151	82,992	03/13/08	20	water allocation = gas allocation	06/13/08	20				185,247	
43047386410000	WRU EIH 7AD-35-8-22	09/26/07	Kmv + Km + Kf + Kd	6,414	1,094,991	80,707	12/12/07	81	0						886,943	0
43047386490000	WRU EIH 9CD-26-8-22	02/14/08	Tw + Kmv + Km + Kf + Kd	6,627	222,201	76,763	06/25/08	10							23,526	
43047386620000	GH 6-20-8-21	12/03/08	Tw + Kmv + Km + Kf + Kd	2,857	454,191	74,293	03/12/09	10							45,419	
43047386630000	WV 6-24-8-21	10/26/08	Tw + Kmv + Km + Kf + Kd	10,747	980,264	73,724	03/12/09	10							98,026	
43047387370000	WV 16C-14-8-21	12/11/08	Tw + Kmv + Km + Kf + Kd	697	325,269	66,243	03/12/09	10							32,527	
43047389900000	GB 1M-4-8-22R (RIGSKID)	08/09/07	Km + Kf + Kd /Tw + Kmv + Km + Kf + Kd (Mowry, not Kd)	14,980	837,936	105,421									NA	
43047389940000	WRU EIH 6D-5-8-23	01/23/08	Kmv + Km + Kf + Kd	16,685	404,910	82,903	04/01/08	0	0	04/13/09	40				52,760	
43047389950000	TU 3-35-7-21	05/24/08	Tw + Kmv + Km + Kf + Kd	2,186	312,441	59,652	08/01/08	10	14	04/13/09	20				29,132	8347
43047390390000	WV 13A-15-8-21	01/09/09	Tw + Kmv + Km + Kf + Kd	2,774	733,566	53,148	03/12/09	10							73,357	
43047390400000	WV 8D-15-8-21	10/21/08	Tw + Kmv + Km + Kf + Kd	4,134	379,506	66,478	03/12/09	10							37,951	
43047390410000	WV 4BD-23-8-21	10/10/08	Tw + Kmv + Km + Kf + Kd	7,281	679,031	68,617	03/23/09	10							67,903	
43047390440000	WV 7BD-23-8-21	08/14/08	Tw + Kmv + Km + Kf + Kd	3,073	365,357	51,202	03/12/09	11.5							42,016	
43047393210000	WV 13AD-8-8-22R(RIGSKID)	11/17/07	Tw + Kmv + Km + Kf + Kd	2,173	375,011	105,444	12/06/07	28	43						105,003	
43047393410000	NBE 8CD-10-9-23	02/23/08	Tw + Kmv + Km + Kf + Kd (Mowry, not Kd)	2,815	294,179	80,542									NA	
43047393460000	NBE 5DD-10-9-23	03/30/08	Kmv + Km + Kf + Kd (Mowry, not Kd)	5,061	137,024	42,909									NA	
43047393480000	NBE 4DD-17-9-23	05/29/08	Tw + Kmv + Km + Kf + Kd	5,377	409,648	30,895	03/12/09	20	water allocation irregular						81,681	
43047393490000	NBE 10CD-17-9-23	04/04/08	Tw + Kmv + Km + Kf + Kd	5,982	175,479	83,995	06/13/08	25							43,872	0
43047393510000	NBE 8BD-26-9-23	04/16/08	Kd (Mowry, not Kd)	20	638,576	2,343									NA	
43047394450000	RW 34-27ADR	02/28/08	Kmv + Km + Kf + Kd / Km + Kf + Kd	7,998	778,803	73,646	03/13/08	20		03/26/08	0	7	03/23/09	10	56,664	
43047396620000	GB 15D-27-8-21	08/03/08	Kmv + Km + Kf + Kd	5,554	648,321	67,056	03/12/09	0							0	
43047396630000	WV 13D-23-8-21	08/08/08	Tw + Kmv + Km + Kf + Kd	6,436	300,794	65,315	04/20/09	25							75,829	
43047396640000	WV 15D-23-8-21	09/24/08	Tw + Kmv + Km + Kf + Kd	3,342	599,951	54,902	03/12/09	20							120,200	
43047403450000	GB 3D-4-8-22R(RIGSKID)	12/07/08	Tw + Kmv + Km + Kf + Kd	8,517	440,210	148,438	03/02/09	10							44,021	

* Abbreviations for Producing Formations: Tw: Wasatch Fm; Kmv: Mesaverde Fm.; Km: Mancos Gp.; Kf: Frontier Fm.; Kd: Dakota Fm.

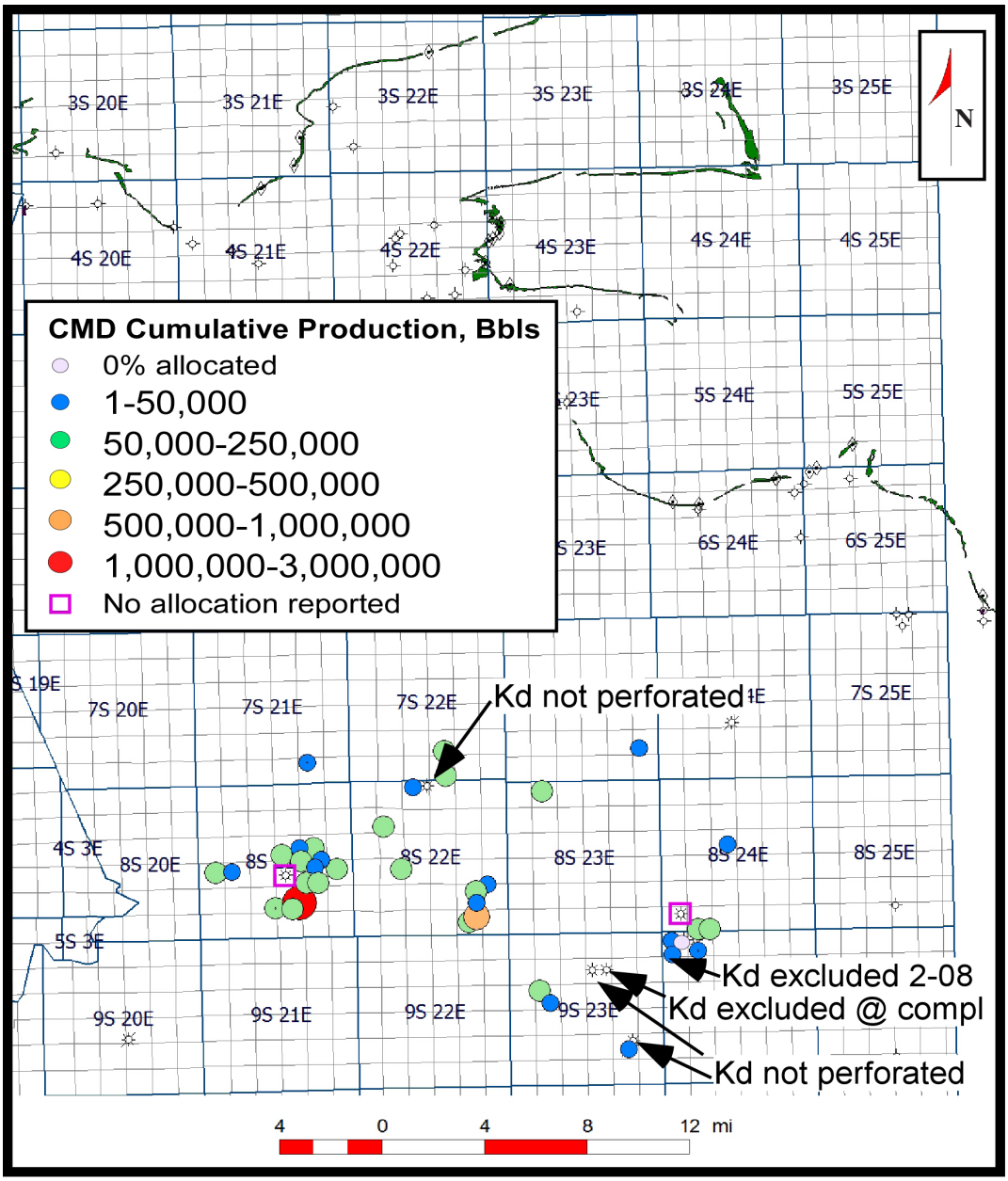

Figure 29. *Map showing location of study area wells with CMD completions (wells with bubbles or magenta squares). The bubbles reflect the cumulative gas produced from the CMD on 9-1-10 as derived from allocations reported to the Utah DOGM.*

GB 9D-27, API 43047349560000, NESE 27-8S-21E

The GB 9D-27 in 27-8S-21E is the only well that is solely completed in the CMD interval. The well was completed in 4-2007 and had produced 2.75 BCF, 630 Bbls oil and 8800 Bbls water as of 9-2010. No stimulation was performed. Figure 30 shows the production profile for the well. We were unable to normalize the production to account for producing days as this value was frequently misreported to the Utah DOGM or incorrectly entered by the Utah DOGM. For example, in May, June, and July of 2008 the well reportedly produced 31, 1, and 24 days, respectively. The corresponding gas production was 188,941, 153,014, and 104,927 MCF. Clearly the well produced more than 1 day in June 2008 but how many days are unknown. The well appears to show linear decline, which indicates matrix storage.

CMD RESERVOIR CHARACTERISTICS

Figure 31 displays the log for the completed interval in well GB 9D-27 located in 27-8S-21E. The log shows that the producing interval has good neutron (PHIN) and density (PHID) cross-over, high resistivity, good separation of shallow and deep resistivity curves that indicates permeability, a blocky

gamma ray signature and slight SP deflection. (The LAS header information did not contain the matrix density that was used to calculate PHID nor was it legible on the scanned raster log at the Utah DOGM website.) The GB 9D-27 was perforated in a single zone with effective reservoir of ~8 ft as indicated by the density porosity curve PHID.

QEP cored the interval equivalent to the producing zone in the GB 9D-27 in the offset GB 15D-27 in SWSE 27-8S-27E. The core captured an upper estuarine interval and a lower fluvial interval. Plate 4 shows the GB 15D-27 log, core description and photomicrographs, the GB 9D-27 log, and a photograph of an analogous outcrop. The core data, porosity, permeability, oil saturation and water saturation, have been depth adjusted +14 ft to correspond with the geophysical logs. The CMD interval in the GB 15D-27 was drilled with oil and this induced oil saturation reflects an interval of permeability.

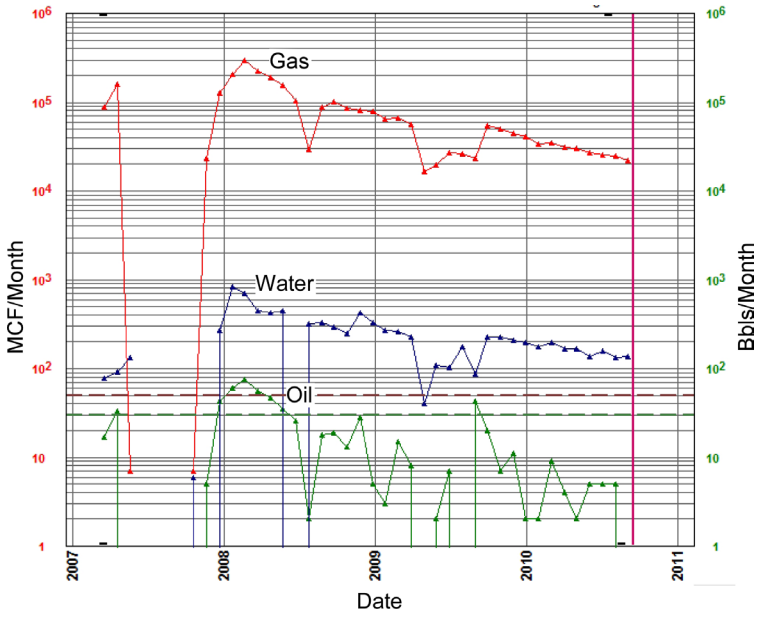

Figure 30. *Monthly production curves for well GB 9D-27 in NESE 27-8S-21E, the sole CMD-only producer.*

We interpret the producing interval, which we named the Kd1 Estuarine sandstone (Plate 4 and Plate 5), as a tidally-dominated estuarine deposit. The reservoir sand is highly bioturbated, and is bounded by shale containing numerous oyster shells and plant material (Figure 32). The top of the reservoir sandstone is heavily rooted, and burrows are identified throughout the interval. This quartz sandstone is clean, well sorted, and very fine grained. The porosity is remnant intergranular, cement is primarily quartz overgrowths, and quartz grains are locally coated with authigenic chlorite (Mark Longman, QEP Resources, personal comm.). The presence of the chlorite is thought to have assisted in the preservation of primary porosity (Thomson, 1982).

The lower sandstone consisted of stacked scours of chert-rich gravels which fined up into trough cross-stratified sandstone. This lower sandstone was intensely cemented with quartz overgrowths and reservoir-quality rock is rare (Figures 33 and 34).

Cross sections were constructed and the Kd1 Estuarine sandstone was correlated (Plate 5). The interval was then mapped and is displayed on both Plate 4 and Plate 5. The sand body strikes NW to SE and parallels some of the channels where orientations were measured in the outcrop. The sandstone attains a maximum gross thickness of 36 ft in 13-8S-21E. We were unable to derive an effective reservoir map as we do not know what perforations are contributing to production in any of the boreholes (besides the GB 9 D-27) and therefore cannot create a model for effective reservoir. It does appear that the presence of chlorite-coated grains is required to preserve reservoir quality rock in the CMD in this area.

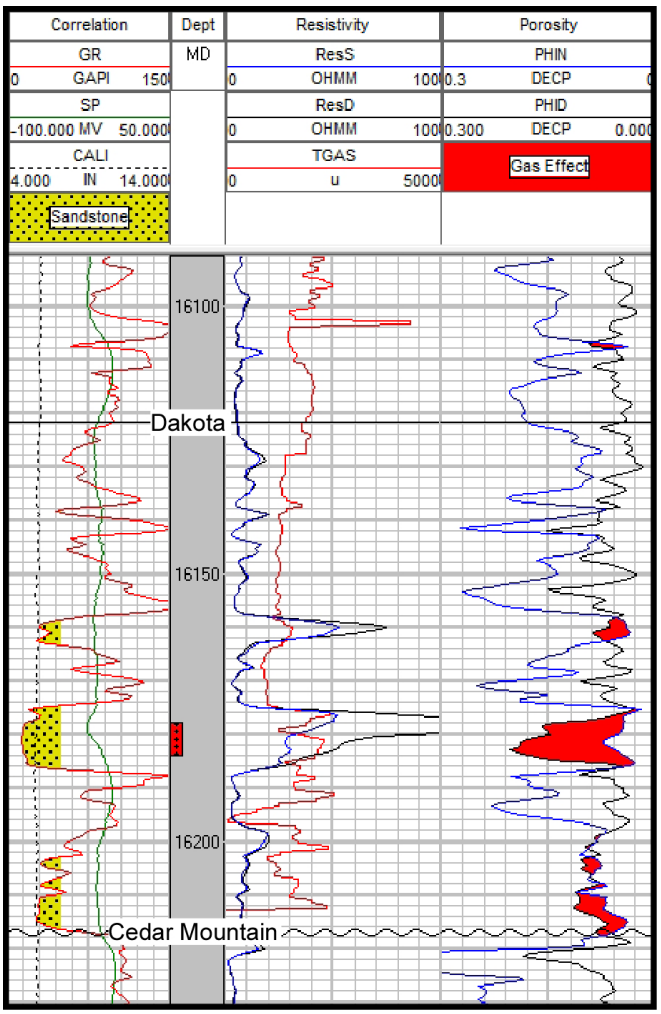

Figure 31. *Log showing the completed interval in the GB 9D-27 well in NE SE 27-8S-21E. The red rectangle in the depth column shows the perforations.*

Figure 32. *Photomicrograph in polarized light from GB 15D-27 core showing oysters and plant debris. The sample is from 16,190.3 (depth adjusted to log) immediately below the Kd1 Estuarine sandstone.*

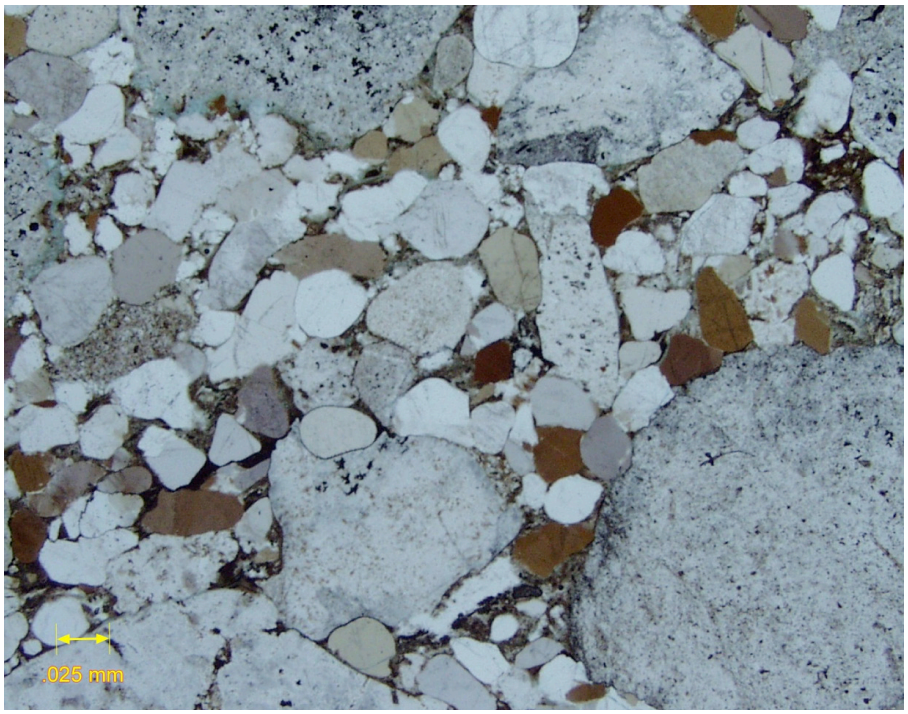

Figure 33. *Photomicrograph of chert-rich gravel in polarized light. The rock is poorly sorted and the small quartz grains have pronounced overgrowths. The mottled gray clasts are the chert; the balance of the grains are quartz. Some clay is in the pore spaces. The photograph is from a log-adjusted depth of 16,204.6 ft. Porosity is 2%.*

CONCLUSIONS

In the northern Uinta Basin, sandstones in the Lower Cretaceous CMD are natural gas reservoirs. The Neocomian-Albian Cedar Mountain Formation consists of the Buckhorn Conglomerate and Ruby Ranch Members. The gravelly-sandy braided fluvial channel deposits of the Buckhorn Conglomerate Member are only present in the southeastern part of the study area, where they reach a maximum thickness of ~100 ft. The unit pinches along a NE-SW trend interpreted as the northwestern edge of a paleovalley that was filled by the Buckhorn Conglomerate Member during the Early Cretaceous. To the NW of this paleovalley, the Ruby Ranch Member sits directly on underlying Jurassic strata. The Ruby Ranch Member consists of 80–150 feet of alluvial mudstone and lenticular fluvial channel sandstones. Current indicators from these channel sands indicate an overall east direction of paleoflow. Channel sandstones are up to 20 ft thick with flow-perpendicular widths of between 250 and 650 ft.

The Dakota Formation in the northern Uinta Basin includes fluvial channel, overbank, estuarine, and marine deposits. Palynomorphs collected from the Dakota Formation indicate a late Albian age of deposition. Based on the architectural arrangement of channel and estuarine/overbank deposits observed in outcrops, the Dakota Formation contains two depositional sequences. The First Dakota sequence (Kd1) is up to 130 ft thick and consists of fluvial channel sandstones and conglomerates, as well as overbank and estuarine sandstone, siltstone, and mudstone. The Kd1 interval was deposited above a regional erosion surface incised as much as 60 ft into the underlying Cedar Mountain Formation. Channelform sandstones and conglomerates are 10–50 ft thick with flow-perpendicular widths of 250–1000 ft. In some cases, vertically-amalgamated channel bodies produce sandstone/conglomerate intervals that are up to 65 ft thick. Cross-bedding orientations from Kd1 channel deposits indicate north-directed paleoflow. The Kd1 also contains broadly tabular estuarine sandstones up to 36 ft thick. While poorly developed in outcrop, these sandstones have been mapped in the subsurface over a 30 mi^2 area.

The Second Dakota sequence (Kd2) is 25–155 ft thick, and contains lithologies similar to the Kd1. The Kd2 was deposited above a surface that is incised up to ~100 ft into the underlying Kd1. In rare instances, the entire Kd1 is eroded and the Kd2 rests directly on the Cedar Mountain Formation. The lower part of the Kd2 is dominated by upward-fining fluvial channel sandstones that are up to 50 ft thick and 1650 ft wide. Where deeply incised into the Kd1, individual channel forms are laterally and vertically amalgamated into complexes that are up to 3300 ft wide and 100 ft thick. Paleocurrent orientations from cross-stratified Kd2 channel deposits indicate primarily north-directed paleoflow. The upper part of the Kd2 consists of up to 50 ft of tidal and marine sandstone, conglomerate, mudstone, and shale. Sandstones in this interval produce continuous sheet-like bodies up to 25 ft thick.

The Mowry Shale overlies the Dakota Formation across the study area. In outcrop, the Mowry Shale is 85–115 ft thick and is composed of siliceous marine shale, mudstone, siltstone, and bentonite beds. These deposits correlate with upward-coarsening shoreface siltstones and sandstones in the subsurface portion of the study area.

Outcrop to subsurface correlation of the CMD interval in the northern Uinta Basin was facilitated by recording outcrop gamma ray logs of study area measured sections. The resulting correlation model allowed confident identification of the tops of the Mowry Shale, Dakota Formation, Cedar Mountain Formation, and Morrison Formation in the subsurface. However, due to lithological similarities, and the erosional truncation and superposition of Kd2 channel complexes with those of the Kd1, the formation is undivided in the subsurface component of this investigation. Overall, the correlation model

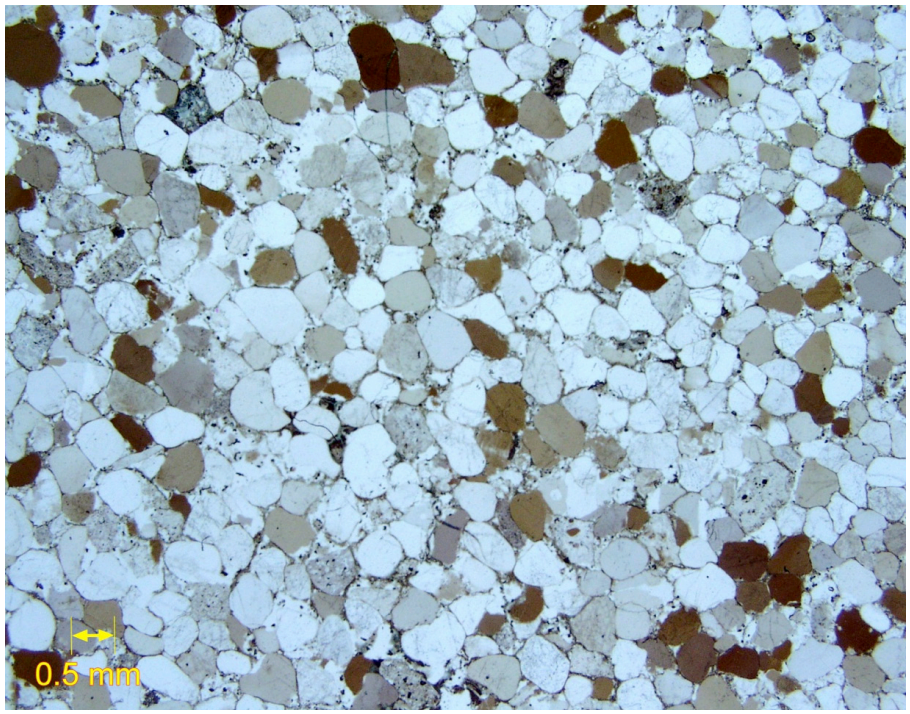

Figure 34. *Photomicrograph in polarized light showing the typical tightly cemented sandstone in the fluvial interval. Quartz overgrowths are dominant and have reduced the porosity to 3.6%. Some clays are in the matrix. The well-rounded grains are thought to be re-worked from Jurassic eolian deposits (Mark Longman, QEP Resources, personal comm.).*

used in this study reinforces the model that was developed by McPherson et al. (2008) for the southern Uinta Basin.

Subsurface correlation of the CMD stratigraphic interval in the northern Uinta Basin was initiated by constructing a correlation envelope and cross lines for all outcrops and available geophysical logs from industry wells in the study area. Tops picked in each well and outcrop location permitted the generation of structure contour and isopach maps for the Mowry Shale, Dakota Formation, Cedar Mountain Formation, Ruby Ranch Member, and Buckhorn Conglomerate Member.

The results of our subsurface correlation also allowed an evaluation of production data and potential reservoir quality from wells that penetrated the CMD in the northern Uinta Basin. The CMD is gas productive in ~40 deep wells in the study area. Within the CMD, most of the production is from the Dakota Formation. Unfortunately, we were unable to quantify CMD interval production because of the production commingling with multiple younger stratigraphic intervals in most studied wells, and the paucity of CMD Fluid Entry Tests reported to Utah DOGM.

For the one well in the study area that had a sole completion in the Dakota Formation, production is apparently from an estuarine sandstone in the lower part of the formation. An evaluation of core data from an adjacent well indicates that high reservoir quality may be controlled by chlorite-coated grains preserving primary porosity in the marine influenced sandstones of the interval. The more ubiquitous fluvial sandstones of the CMD appear to have low porosities and permeabilities due to the presence of well-developed quartz overgrowth cements.

ACKNOWLEDGMENTS

This project was funded by a Natural Gas Reservoir Characterization Grant from the Utah Geological Survey. Additional support was provided by the Miami University Department of Geology Rocky Mountain Petroleum Geology Research Fund, the Miami University Undergraduate Summer Scholar Program, and graduate student research grants from the Geological Society of America, American Association of Petroleum Geologists, and Colorado Scientific Society. Interpretation software used at Miami University was supplied by the Landmark Graphics Corporation University Software Grant Program. MJ Systems provided raster log files to Miami University. Field discussions, photographs, and editorial assistance provided by Robert Ressetar of the Utah Geological Survey were instrumental in the success of the project. Mike Murphy and the DNR staff at Steinaker State Park were instrumental in expediting permits for the study. Special thanks goes to Mark Longman of QEP Resources for his insights into the Dakota Formation of the northern Uinta Basin, and for providing the core data and digital well logs used in the study.

REFERENCES

Aubrey, W.M., 1998, A newly discovered, widespread fluvial facies and unconformity marking the Upper Jurassic/Lower Cretaceous boundary, Colorado Plateau, *in* Carpenter, K., Chure, D., and Kirkland, J.I., editors, The Upper Jurassic Morrison Formation—an interdisciplinary study, Part I: Modern Geology, v. 22, p. 209–233.

Boersma, J.R., and Terwindt, J.H.J., 1981, Neap-spring tide sequences of intertidal shoal deposits in a mesotidal estuary: Sedimentology, Vol. 28, no. 2, p. 151–170..

Byers, C.W., and Larson, D.W., 1979, Paleoenvironments of Mowry Shale (Lower Cretaceous), western and central Wyoming: American Association of Petroleum Geologists Bulletin, v. 63, p. 354–375.

Currie, B.S., 1997, Sequence stratigraphy of nonmarine Jurassic-Cretaceous rocks, central Cordilleran foreland basin: Geological Society of America Bulletin, v. 109, p. 1206–1222.

Currie, B.S., 1998, Upper Jurassic-Lower Cretaceous Morrison and Cedar Mountain Formations, NE Utah-NW Colorado—relationships between nonmarine deposition and early Cordilleran foreland basin development: Journal of Sedimentary Research, v. 68, p. 632-652.

Currie, B.S., 2002, Structural configuration of the Late Jurassic-Early Cretaceous Cordilleran foreland-basin system and Sevier thrust belt, Utah and Colorado: Journal of Geology, v. 110, no. 6, p. 697–718.

Currie, B.S., Dark, J.P., McPherson, M.L., and Pierson, J.S., 2008a, Fluvial channel architecture of the Albian-Cenomanian Dakota Formation, southern Uinta Basin, *in* Longman, M.A., and Morgan, C.D., editors, Hydrocarbon systems and production in the Uinta Basin, Utah: Rocky Mountain Association of Geologists and Utah Geologic Association Publication 37, p. 65–79.

Currie, B.S., McPherson, M.L., Dark, J.P., and Pierson, J.S., 2008b, Reservoir characterization of the Cretaceous Cedar Mountain and Dakota formations, southern Uinta Basin—year two report: Utah Geological Survey Open-File Report 516, 117 p.

Dalrymple, R.W., Zaitlin, B.A., and Boyd, R., 1992, Estuarine facies models— conceptual basis and stratigraphic implications: Journal of Sedimentary Research, v. 62, p. 1130–1146.

Dark, J.P, Currie, B.S., McPherson, M.L., Rakovan, J., and Marchlewski, T.A., 2008, Structural, lithological and diagenetic controls on Dakota Formation economic gas production within the greater San Arroyo gas field, Utah, *in* Longman, M.A., and Morgan, C.D., editors, Hydrocarbon systems and production in the Uinta

Basin, Utah: Rocky Mountain Association of Geologists and Utah Geologic Association Publication 37, p. 179–208.

Davis, R.H., and Byers, C.W., 1989, Shelf sandstones in the Mowry Shale— Evidence for deposition during Cretaceous sea level falls: Journal of Sedimentary Petrology, v. 59, p. 548–560.

Demko, T.M., Currie, B.S., and Nicoll, K.A., 2004, Regional paleoclimatic and stratigraphic implications of paleosols and fluvial-overbank architecture in the Morrison Formation (Upper Jurassic), Western Interior, U.S.A.: Sedimentary Geology, v. 167, p. 117–137.

Gradstein, F.M., Ogg, J., and Smith, A., 2004, A geologic time scale 2004: Cambridge University Press, 610 p.

Kirkland, J.I., 2005, Utah's newly recognized dinosaur record from the Early Cretaceous Cedar Mountain Formation: Utah Geological Survey, Survey Notes, v. 33, no. 1, p. 1–5.

Kirkland, J.I., and Madsen, S.K., 2007, The Lower Cretaceous Cedar Mountain Formation, eastern Utah—the view up an always interesting learning curve: Geological Society of America Rocky Mountain Section Meeting Field Trip Guide Book, 108 p.

Ludvigson, G.A., Joeckel, R.M., Gonzalez, L.A., Gulbranson, E.L., Rasbury, E.T., Hunt, G.J., Kirkland, J.I., and Madsen, S.K., 2010, Correlation of Aptian-Albian carbon isotope excursions in continental strata of the Cretaceous foreland basin of eastern Utah: Journal of Sedimentary Research, v. 80, p. 955–974.

McPherson, M.L., Currie, B.S., and Pierson, J.S., 2006, Reservoir characterization of the Cretaceous Cedar Mountain and Dakota Formations, Southern Uinta Basin—year one report, Utah Geological Survey Open-file Report 492, 99 p.

McPherson, M.L., Currie, B.S., Dark, J.P., and Pierson, J.A., 2008, Outcrop-to-subsurface correlation of the Cretaceous Cedar Mountain and Dakota Formations, southern Uinta Basin, *in* Longman, M.A., and Morgan, C.D., editors, Hydrocarbon systems and production in the Uinta Basin, Utah: Rocky Mountain Association of Geologists and Utah Geologic Association Publication 37, p. 43–63.

Molenaar, C.M., and Wilson, B.W., 1990, The Frontier Formation and associated rocks of northeastern Utah and northwestern Colorado: U.S. Geological Survey Bulletin 1787-M, 21 p.

Molenaar, C.M., and Cobban, W.A., 1991, Middle Cretaceous stratigraphy on the south and east sides of the Uinta Basin, northeastern Utah and northwestern Colorado: U.S. Geological Survey Bulletin 1787-P, 34 p.

Oboh-Ikuenobe, F.E., Benson, D.G., Scott, R.W., Holbrook, J.M., Evetts, M.J., and Erbacher, J., 2007, Re-evaluation of the Albian-Cenomanian boundary in the U.S. Western Interior based on dinoflagellate cysts: Review of Paleobotany and Palynology, v. 144, p. 77–97.

Obradovich, J.D., 1993, A Cretaceous time scale, *in* Caldwell, W.G.E., and Kauffman, E.G., editors, Evolution of the Western Interior Basin: Geological Association of Canada Special Paper 39, p. 379–396.

Pierson, J.S., 2009, Stratigraphy and palynology of the Albian-Cenomanian Dakota Formation and Mowry Shale, Uinta Basin, Utah and Colorado: Oxford, Ohio, Miami University, M.S. thesis, 65 p.

Quigley, M.D., 1959, Correlation of the Dakota-Cedar Mountain-Morrison sequence along the Douglas Creek Arch, *in* Haun, J.D. and Weimer, R.J., editors, Symposium on Cretaceous rocks of Colorado and adjacent areas: 11th Field Conference Guidebook, Rocky Mountain Association of Geologists, p. 13–17.

Roca, X., and Nadon, G.C., 2007, Tectonic control and the sequence stratigraphy of nonmarine retro-arc foreland basin fills—insights from the Upper Jurassic of central Utah, U.S.A.: Journal of Sedimentary Research, v. 77, p. 239–255.

Ryer, T.A., McClurg, J.J., and Muller, M.M., 1987. Dakota–Bear River paleoenvironments, depositional history and shoreline trends—implications for foreland basin paleotectonics, southwestern Green River basin and southern Wyoming overthrust belt, *in* Miller, W.R., editor, The thrust belt revisited: 38th Field Conference Guidebook, Casper, Wyoming Geological Association, p. 179–206.

Scott, R.W., Oboh-Ikuenobe, F.E., Benson, D.G., Jr., and Holbrook, J.M., 2009, Numerical age calibration of the Albian/Cenomanian boundary: Stratigraphy, v. 6, p. 17–32.

Sharp, J.V.A., 1963, Unconformities within basal marine Cretaceous rocks of the Piceance Basin, Colorado: Boulder, University of Colorado, Ph.D. dissertation, 170 p.

Sprinkel, D.A., Madsen, S.K., Kirkland, J.I., Waanders, G.L., and Hunt, G.J., 2012, Cedar Mountain and Dakota Formations around Dinosaur National Monument—evidence of the first incursion of the Cretaceous Western Interior Seaway into Utah: Utah Geological Survey Special Study 143, 21 p.

Stokes, W.L., 1952, Lower Cretaceous in Colorado Plateau: American Association of Petroleum Geologists Bulletin, v. 36, p. 1766–1776.

Thomson, A., 1982, Preservation in porosity in the deep

Woodbine/Tuscaloosa Trend, Louisiana: Journal of Petroleum Technology, v. 34, p. 1156–1162.

Vaughn, R.L., and Picard, M.D., 1976, Stratigraphy, sedimentology, and petroleum potential of the Dakota Formation, northeastern Utah, *in* Hill, J.G., editor, Geology of the Cordilleran Hingeline, Rocky Mountain Association of Geologists, p. 267–279.

Young, R.G., 1960, The Dakota Group of the Colorado Plateau: American Association of Petroleum Geologists Bulletin, v. 44, p. 56–194.